C.P. No. 13
(12329)
A.R.C. Technical Report

MINISTRY OF SUPPLY

AERONAUTICAL RESEARCH COUNCIL
CURRENT PAPERS

# The Viscid Flow of Air in a Narrow Slot

*By*

G. L. Shires



LONDON : HIS MAJESTY'S STATIONERY OFFICE

1950

Price 2s 6d net

Memorandum No. M.46.

December, 1948.

NATIONAL GAS TURBINE ESTABLISHMENT

# The Viscid Flow of Air in a Narrow Slot

- by -

G.L. Shires.

SUMMARY

The properties of the viscid flow of air in a rectangular slot having a width large in comparison with its depth are investigated. The results of various tests are found to verify theoretical and empirical relationships between the pressure distribution in the slot, the air mass flow and temperature, and the slot dimensions. Both laminar and turbulent flows are considered.

CONTENTS

| | | Page |
|---|---|---|
| 1.0 | Introduction | 1 |
| 2.0 | The Equations of Viscid Flow | 2 |
| | 2.1 The Theoretical Equation for Laminar Flow | 2 |
| | 2.2 The Empirical Equation using the Resistance Coefficient | 3 |
| | 2.3 Solutions for Three Particular Cases | 5 |
| 3.0 | The Apparatus and the Method of Testing | 7 |
| 4.0 | The Analysis of the Test Results | 7 |
| | 4.1 Case 1. Constant Cross Section | 7 |
| | 4.2 Case 2. Constant Depth and Increasing Width | 8 |
| | 4.3 Case 3. Constant Width and Increasing Depth | 9 |
| 5.0 | Conclusions | 10 |
| List of Illustrations | | 10 |
| List of Appendices | | 11 |
| References | | 11 |
| Appendices I to IV | | 12 - 16 |
| Figures 1 to 13 | | |

## 1.0 Introduction

The three forces affecting the flow of air in a slot are the pressure force, the force due to viscosity, and the force required to accelerate or deccelerate the fluid. If, however, the depth of the slot is very small, the viscid force and the pressure force are very large, and in comparison the inertia force is small enough to be neglected. This being so, the viscid force is equated to the pressure force and a simple theoretical equation relating the pressure distribution, the air temperature, the mass flow and the slot dimensions is obtained for steady laminar flow. To derive a similar equation for turbulent flow the problem is considered in

ADDENDUM TO A.R.C. CURRENT PAPER No. 13

## Mach Number

Although the above analysis is concerned with the pressure drop along a narrow rectangular slot the experimental results may also be expressed in terms of Mach number, M. For this purpose the mean velocity based on mass flow, $\bar{u} = \frac{G}{\rho . a . h}$, is taken as representative and values of M calculated from the expression -

$$M = \frac{\bar{u}}{\sqrt{\gamma g R T}} = \sqrt{\frac{RT}{\gamma g}} \cdot \frac{G}{p . a . h} .$$

Over the test length the Mach number was always low and variations of temperature were negligible. Hence, over this section,

$$M \doteq \sqrt{\frac{RT_o}{\gamma g}} \cdot \frac{G}{p . a . h} ,$$

where $T_o$ is the reservoir temperature. Typical curves of static pressure, p, and Mach number, M, over the test length of a parallel sided rectangular slot (case 1.) are shown as full lines in Fig. 14(a).

In the last inch of slot there is a large drop in pressure and density and hence a rapid acceleration. In this length the variation of temperature cannot be neglected. If adiabatic flow is assumed in this part of the slot the exit Mach number, $M_e$, can be calculated for case 1, from equations given by Kestin and Oppenheim.* These can be reduced to the expression:

$$\frac{\lambda L}{D} = \frac{1}{4\gamma} \left\{ \left[ \frac{1}{M_1{}^2} - \frac{\gamma+1}{2} \log_e \left( \frac{1}{M_1{}^2} + \frac{\gamma+1}{2} \right) \right] - \left[ \frac{1}{M_2{}^2} - \frac{\gamma+1}{2} \log_e \left( \frac{1}{M_2{}^2} + \frac{\gamma-1}{2} \right) \right] \right\}$$

where subscripts 1 and 2 denote two positions separated by a distance L. The resistance coefficient λ is assumed to be the same all along the slot, since the Reynolds Number is constant, and its value is calculated from measurements in the test length. The calculation of the exit Mach number, $M_e$, is in effect an extrapolation of the curves of Mach number in the test length with the assumption of adiabatic expansion in the last inch. Such extrapolation is, of course, necessary since the pressure just inside the slot exit is not always atmospheric. When the slot is choked it may be much higher as in case (b) in Fig. 14(a). Case (a) is unchoked.

When $M_e$ is plotted against the mass flow, Fig. 14(b), it attains a constant value, not necessarily equal to unity, indicating that choking conditions were reached, with the four larger clearances. The fact that $M_e$ does not become unity may be due to it being based on the mean velocity whereas the exit velocity profile was probably not uniform and choking probably occurred when the maximum velocity reached the local sonic value. If this is true then the apparent Mach number, $M_e$, corresponding to choking the exit is effectively a profile factor. The reduction of the choking value of $M_e$ with decreasing clearance seems to indicate the truth of this assumption.

* J. Kestin, A.K. Oppenheim - The Calculation of Compressible Fluid Flow by the Use of a Generalised Entropy Chart (Equations 17 and 65a). - Inst. of Mech. Eng., Proc. 1948, Vol. 159, War Emergency Issue No. 43.

terms of the resistance coefficient, $\lambda$, and the Reynold's number, Re.

The relationship between $\lambda$ and Re for the flow of an incompressible fluid in pipes and slots has been a subject of research for many years, but little information is available concerning the flow of a compressible fluid subject to large changes in pressure and therefore to large changes in density. Experiments have therefore been performed in slots of various shapes on the flow of air subject to such changes, and the results, when expressed in terms of the parameters $\lambda$ and Re, are compared with the results of experiments with incompressible fluids carried out by Blasius (Ref. 1).

## 2.0 The Equations of Viscid Flow

The theory of the steady laminar flow of a compressible viscid fluid in a slot the cross section of which is constant, or changing very slowly, may be developed from first principles, the method being an extension of that used in hydrodynamic theory with a function of temperature and pressure replacing the density term. For turbulent flow use is made of the concept of the resistance coefficient, $\lambda$, where

$$\lambda = \frac{\tau}{\frac{1}{2}\rho\bar{u}^2}$$

$\tau$ being the "skin friction" per unit of surface area in contact with the fluid, $\bar{u}$ the spatial mean velocity, and $\rho$ the density of the fluid. The relationship between $\lambda$ and the Reynolds number, $R_e$, based on the hydraulic mean depth for turbulent flow is given empirically by Blasius (Ref. 1) as

$$\lambda_T = \frac{0.079}{Re^{\frac{1}{4}}}$$

and this value can be used to develop an equation corresponding to that obtained theoretically for laminar flow.

The assumptions made in the derivation of the equations of flow are the same in both cases. The force required to accelerate or deccelerate the fluid is assumed to be negligible; the pressure distribution over any cross section is assumed to be uniform, and the temperature of the air as it flows along the slot is assumed to be constant.

### 2.1 The Theoretical Equation for Laminar Flow

Consider an elementary volume of the fluid, as shown in Fig.1a, situated at a point in the slot.

The inertia term being neglected, the resulting forces acting on the element in the direction of the x-axis, which is the direction of flow, are:-

The viscid force $= \frac{\partial s}{\partial y} \cdot \delta y \cdot \delta x \cdot \delta z$ and

The pressure force $= -\frac{\partial p}{\partial x} \cdot \delta x \cdot \delta y \cdot \delta z$, where s is the shearing stress in the fluid, p is the absolute pressure, $\rho$ is the density, and u is the velocity in the x direction.

By equating these forces we obtain the relationship

$$\frac{\partial p}{\partial x} = \frac{\partial s}{\partial y}$$

which, since $s = \mu \cdot \frac{\partial u}{\partial y}$ and $\frac{\partial s}{\partial y} = \mu \cdot \frac{\partial^2 u}{\partial y^2}$, may be written as

$$\frac{\partial p}{\partial x} = \mu \cdot \frac{\partial^2 u}{\partial y^2} \qquad \text{.........} \ ..(1)$$

For the flow of a compressible fluid in a slot having two closely adjacent walls it is assumed that

$$\frac{\partial p}{\partial y} = \frac{\partial p}{\partial z} = 0$$

For the narrow slot, therefore, equation (1) becomes

$$\frac{dp}{dx} = \mu \cdot \frac{\partial^2 u}{\partial y^2} \qquad \text{............(2)}$$

Integrating this with respect to y we obtain

$$u = \frac{1}{2\mu} \cdot \frac{dp}{dx} \cdot y^2 + C_1 . y + C_2$$

The depth of the slot is h, where h is a function of x, and, since u = 0 when y = 0 or y = h, we have

$$C_1 = -\frac{h}{2\mu} \cdot \frac{dp}{dx} \text{ , and } C_2 = 0$$

Hence

$$u = \frac{y^2 - hy}{2\mu} \cdot \frac{dp}{dx} \qquad \text{................(3)}$$

and this is a parabolic form of velocity profile.

The mean velocity at any cross section is

$$\bar{u} = \frac{1}{h} \cdot \int_0^h u \, dy$$

$$= \frac{1}{h} \cdot \frac{dp}{dx} \cdot \int_0^h \frac{y^2 - hy}{2\mu} \cdot dy$$

$$= -\frac{dp}{dx} \cdot \frac{h^2}{12\mu} \qquad \text{................(4)}$$

If the width of the slot be denoted by $\sigma$, where $\sigma$ is a function of x, the mass flow along the slot is then given by

$$G = \rho \cdot \sigma \cdot h \cdot \bar{u}$$
$$= -\frac{\rho \cdot \sigma \cdot h^3}{12\mu} \cdot \frac{dp}{dx}$$

From which we have

$$\frac{dp}{dx} = -\frac{12 \cdot \mu \cdot G}{\rho \cdot \sigma \cdot h^3}$$

and, substituting in this equation the value $\rho = \frac{p}{RT}$, we obtain

$$\frac{dp}{dx} = -\frac{12\mu \cdot RT \cdot G}{p \cdot \sigma \cdot h^3}$$

$$\text{or } p \cdot dp = -\frac{12\mu \cdot RT \cdot G}{\sigma \cdot h^3} \cdot dx \qquad \text{..............(5)}$$

If T, $\sigma$, and h are known functions of x, this equation can be integrated and the theoretical pressure distribution so obtained.

2.2 The Empirical Equation using the Resistance Coefficient

Fig. 1b shows an elementary volume of the fluid between the two plates, its length in the x direction being infinitesimally small and its width in the z direction being unity. When considering the forces acting on this element the assumptions made are that:-

1) The kinetic energy changes involved are negligible,

2) $\frac{\partial p}{\partial y} = \frac{\partial p}{\partial z} = 0.$

The force, F, resisting the motion of the fluid may be considered as due to the friction acting at the surface of contact between the fluid and the walls. If the "skin friction" per unit area of "wetted surface" be denoted by $\tau$, then

$$F = \tau . (AE) . \cos\theta + \tau . (CD) . \cos\phi$$

i.e.
$$F = 2\tau . \delta x.$$

The pressure force acting in the direction of motion is given by

$$P = p . h + (p + \frac{1}{2}\frac{dp}{dx} . \delta x) \left\{(AB) \sin\theta + (CD) \sin\phi\right\}$$

$$- (p + \frac{dp}{dx} . \delta x)(h + \frac{\partial h}{\partial x} . \delta x)$$

$$= p . h + (p + \frac{1}{2}\frac{dp}{dx} . \delta x) \left\{\frac{\partial h}{\partial x} . \delta x\right\} - (p + \frac{dp}{dx} . \delta x)(h + \frac{\partial h}{\partial x} . \delta x)$$

which reduces to

$$P = - h . \frac{dp}{dx} . \delta x$$

Equating these two forces F and P we have

$$2\tau . \delta x = - h . \frac{dp}{dx} . \delta x$$

or
$$\frac{dp}{dx} = - \frac{2\tau}{h}$$

Now $\tau/\frac{1}{2}\rho\bar{u}^2$ is the resistance coefficient, $\lambda$, and hence

$$\therefore \frac{dp}{dx} = - \frac{\lambda . \rho . \bar{u}^2}{h} \quad\quad ..................(6)$$

The coefficient, $\lambda$, is dependent on the Reynolds number, Re, apertaining. For laminar flow the value of $\lambda_L$ which gives an equation identical with (5) in section 2.1 is

$$\lambda_L = \frac{24}{Re}$$

For turbulent flow $\lambda_T$ is given empirically by Blasius as

$$\lambda_T = \frac{0.079}{Re^{\frac{1}{4}}}$$

Substituting $\lambda_L$ in equation (6), we have

$$\frac{dp}{dx} = - \frac{24}{Re} . \frac{\rho . \bar{u}^2}{h} = - \frac{24}{Re} . \frac{G^2}{\rho . a^2 . h^3}$$

where
$$Re = \frac{2 h . \bar{u} . \rho}{\mu} = \frac{2 G}{a . \mu}$$

Hence
$$\frac{dp}{dx} = - \frac{12\,\mu\,.\,G}{\sigma\,.\,h^3\,.\,\rho}$$

or
$$\rho\,.\,d\rho = - \frac{12\,\mu\,.\,RT\,.\,G\,.\,dx}{\sigma\,.\,h^3}$$

which is the same as equation (5).

To obtain the corresponding equation for turbulent flow we substitute in equation (6) the value of $\lambda_T$.

$$\frac{dp}{dx} = - \frac{0.079}{Re^{\frac{1}{4}}}\,.\,\frac{\rho\,.\,u^2}{h} = - \frac{0.079}{Re^{\frac{1}{4}}}\,.\,\frac{G^2}{\rho\,.\,\sigma^2\,.\,h^3}$$

$$= - \frac{0.079}{(2)^{\frac{1}{4}}}\,.\,\frac{\sigma^{\frac{1}{4}}\,.\,\mu^{\frac{1}{4}}}{G^{\frac{1}{4}}}\,.\,\frac{G^2}{\rho\,.\,\sigma^2\,.\,h^3}$$

$$= - \frac{0.067\ \mu^{\frac{1}{4}}\,.\,G^{\frac{7}{4}}}{h^3\,.\,\sigma^{\frac{7}{4}}\,.\,\rho}$$

$$\text{or}\quad p\,.\,dp = - \frac{0.067\ \mu^{\frac{1}{4}}\,.\,RT\,.\,G^{\frac{7}{4}}}{\sigma^{\frac{7}{4}}\,.\,h^3}\,.\,dx \qquad \text{.................(7)}$$

2.3 Solutions for Three Particular Cases

The general equations, (5) and (7), can be integrated if $\sigma$, h, and T are known as functions of x. For the three types of slot illustrated in Fig. 2 the integrations have been performed on the assumption that the temperature, T, is constant along the slot.

Case 1. $\sigma$ and h constant

The integration of equation (5) gives in this case the following result for steady laminar flow.

$$p^2 = \text{constant} - \left(\frac{24\,\mu\,.\,RT\,.\,G}{\sigma\,.\,h^3}\,.\,x\right) \qquad \text{............(8)}$$

$$\text{or}\quad p_1{}^2 - p_2{}^2 = \frac{24\,\mu\,.\,RT\,.\,G}{\sigma\,.\,h^3}(x_2 - x_1) \qquad \text{.............(9)}$$

On integrating equation (7), we obtain for turbulent flow

$$p^2 = \text{constant} - \left(\frac{0.133\ \mu^{\frac{1}{4}}\,.\,RT\,.\,G^{\frac{7}{4}}}{\sigma^{\frac{7}{4}}\,.\,h^3}\,.\,x\right) \qquad \text{........(10)}$$

$$\text{or}\quad p_1{}^2 - p_2{}^2 = \frac{0.133\ \mu^{\frac{1}{4}}\,.\,RT\,.\,G^{\frac{7}{4}}}{\sigma^{\frac{7}{4}}\,.\,h^3}(x_2 - x_1) \qquad \text{...........(11)}$$

Case 2. h constant and $\sigma = \alpha.\ x$

If the frictional effect of the two side walls is neglected, the flow in this case is analogous to the radial flow between two uniformly spaced circular flat plates and by symmetry the pressure at any radius is constant.

Provided, therefore, that the divergence is small the pressure in any plane perpendicular to the axis is approximately constant and equations (5) and (7) may be applied. By substituting in these equations $a = \alpha . x$, we obtain for laminar flow

$$p \, . \, dp = - \frac{12 \mu \, . \, RT \, . \, G}{\alpha \, . \, h^3} \, . \, \frac{dx}{x}$$

which when integrated becomes

$$p^2 = \text{constant} - \left( \frac{24 \mu \, . \, RT \, . \, G}{\alpha \, . \, h^3} \, . \, \log_e x \right) \quad \ldots\ldots\ldots\ldots(12)$$

$$\text{or } p_1^2 - p_2^2 = \frac{24 \mu \, . \, RT \, . \, G}{\alpha \, . \, h^3} \, . \, \log_e \frac{x_2}{x_1} \quad \ldots\ldots\ldots\ldots(13)$$

and, for turbulent flow,

$$p \, . \, dp = - \frac{0.067 \mu^{\frac{1}{4}} \, . \, RT \, . \, G^{\frac{7}{4}}}{\alpha^{\frac{7}{4}} \, . \, h^3} \, . \, \frac{dx}{x^{\frac{7}{4}}}$$

which when integrated becomes

$$p^2 = \text{constant} + \left( \frac{0.178 \mu^{\frac{1}{4}} \, . \, RT \, . \, G^{\frac{7}{4}}}{\alpha^{\frac{7}{4}} \, . \, h^3} \, . \, \frac{1}{x^{\frac{3}{4}}} \right) \quad \ldots\ldots\ldots\ldots(14)$$

$$\text{or } p_1^2 - p_2^2 = \frac{0.178 \mu^{\frac{1}{4}} \, . \, RT \, . \, G^{\frac{7}{4}}}{\alpha^{\frac{7}{4}} \, . \, h^3} \left\{ \frac{1}{x_1^{\frac{3}{4}}} - \frac{1}{x_2^{\frac{3}{4}}} \right\} \quad \ldots\ldots\ldots\ldots(15)$$

Case 3. Constant Width and Increasing Depth

As the deviation of the two plane surfaces is very small, the components of velocity perpendicular to the axis of the slot must also be very small, and the pressure distribution over any cross section is, therefore, assumed to be uniform.

For laminar flow, by substituting $h = \beta \, . \, x$ in equation (5), we obtain

$$p \, . \, dp = - \frac{12 \mu \, . \, RT \, . \, G}{a \, . \, \beta^3} \, . \, \frac{dx}{x^3}$$

and when integrated this becomes

$$p^2 = \text{constant} + \left( \frac{12 \mu \, . \, RT \, . \, G}{a \, . \, \beta^3} \, . \, \frac{1}{x^2} \right) \quad \ldots\ldots\ldots\ldots(16)$$

$$\text{or } p_1^2 - p_2^2 = \frac{12 \mu \, . \, RT \, . \, G}{a \, . \, \beta^3} \left\{ \frac{1}{x_1^2} - \frac{1}{x_2^2} \right\} \quad \ldots\ldots\ldots\ldots(17)$$

By the same substitution in equation (7) we have, for turbulent flow,

$$p \, . \, dp = - \frac{0.067 \mu^{\frac{1}{4}} \, . \, RT \, . \, G^{\frac{7}{4}}}{a^{\frac{7}{4}} \, . \, \beta^3} \, . \, \frac{dx}{x^3}$$

which when integrated gives

$$p^2 = \text{constant} + \left( \frac{0.067 \mu^{\frac{1}{4}} \, . \, RT \, . \, G^{\frac{7}{4}}}{a^{\frac{7}{4}} \, . \, \beta^3} \, . \, \frac{1}{x^2} \right) \quad \ldots\ldots\ldots\ldots(18)$$

$$\text{or} \quad p_1^2 - p_2^2 = \frac{0.067\,\mu^{\frac{1}{4}} \,.\, RT \,.\, G^{\frac{7}{4}}}{\sigma^{\frac{7}{4}} \,.\, \beta^3} \left\{\frac{1}{x_1^2} - \frac{1}{x_2^2}\right\} \qquad \ldots\ldots\ldots\ldots\ldots(19)$$

## 3.0 The Apparatus and the Method of Testing

The apparatus, as shown in Fig. 3, consisted essentially of two flat steel plates separated by thin strips of steel arranged so as to form a passage of the required shape. The two plates were made $\frac{7}{8}$" thick to prevent any appreciable bending, and, after the upper one had been case hardened, the surfaces forming the horizontal walls of the slot were carefully ground and tested against an optical "flat". The maximum deviation from the plane, as estimated by counting the interference fringes, was about $50 \,.\, 10^{-6}$ inches. Between the two plates the slot was bounded on each side by strips of steel, which in the case of the slots of constant depth were of single thickness but which for slots of varying depth were overlapped in the form of steps. When the block was assembled and firmly clamped together a sealing compound was applied externally to all the joints.

During the tests compressed air at a recorded temperature, T, passed through a metering section and into the sharp edged rectangular reservoir in the upper plate. From there it flowed along the rectangular passage between the two plates to atmosphere, the static pressure being recorded at intervals of $\frac{1}{4}$" along the axis. A line of 7 pressure tappings across the slot at right angles to the axis was used as a check upon the setting of the block, since any inclination of the two surfaces in a plane perpendicular to the axis would result in an assymmetrical pressure distribution over these 7 points. The pressure distribution at this cross section was found to be uniform as assumed in the theory.

The procedure for each test was the same and consisted of two parts. The first was the recording of the axial pressure distribution for various values of the reservoir pressure, $p_0$, and the analysis of these results. It was invariably found that the pressure distribution over the central 3" length of slot comformed to the corresponding theoretical form and that this length could be considered as a suitable test length. The second part of the procedure involved an investigation of the relationship between the air mass flow, G, in the slot and the pressures $p_1$ and $p_2$, where $p_1$ denotes the pressure at the upstream end and $p_2$ the pressure at the downstream end of the test length.

## 4.0 The Analysis of the Test Results

The aim of the tests was to check the validity of the formulae developed in sections 2.1 and 2.2, and, where possible, to determine the relationship between the resistance coefficient, $\lambda$, and the Reynold's number, Re. Since the equations involve both the width, $\sigma$, and the depth, h, as variables, it was necessary as an overall check to use three types of slot, one with a constant cross section, one with a varying width, and one with a varying depth. Equations (8) to (19) apply to the three types of slot used and are compared in the following pages with the test results obtained.

### 4.1 Case 1. Constant Cross Section

Tests were made with six slots having a width, $\sigma$, of 1.75" and a depth, h, of approximately 0.0020", 0.0030", 0.0040", 0.0050", 0.0058", and 0.0093".

Fig. 4 shows the axial pressure distributions as recorded for two of the slots, the distributions obtained with the other four slots being of the same form. When the square of the absolute pressure, $p^2$, is plotted against the axial distance, x, a series of straight lines are obtained over the central 3" length of the slot, the form of the theoretical relationship between p and x being thus verified.

The slope of each of these straight lines, $\left(\frac{p_1^2 - p_2^2}{x_2 - x_1}\right)$, is a measure of the resistance to flow and is plotted logarithmically against the corresponding mass flow, G, in Fig. 5. Here, the six curves represent the results for the six slots investigated and, since outside the transition zone each set of results can be represented by two straight lines, the relationship between the pressure drop and the mass flow is clearly of the form

$$\frac{p_1^2 - p_2^2}{x_2 - x_1} = \text{Constant} \; . \; G^n \; .$$

The constant in this equation is different for laminar and for turbulent flow as is also the index n, which for laminar flow is 1.0 and for turbulent approximately 1.75. The non-linear part of the curve represents the transition from laminar to turbulent flow.

The experimental results are also shown as points in Fig. 6, together with the theoretical curves obtained by substituting in equations (9) and (11) the slot dimensions and the air temperature. The difference between the corresponding calculated and measured values of $\left(\frac{p_1^2 - p_2^2}{x_2 - x_1}\right)$ as a percentage of the measured value, is with one exception less than 5% for laminar flow and less than 10% for turbulent flow. The larger overall discrepancy in the case where h = 0.0030" is probably due to a small error in the measurement of h.

To complete the picture a graph is given in Fig. 7 of the resistance coefficient, $\lambda$, against the Reynold's number, Re, where $\lambda$ and Re are calculated according to the equations derived in Appendix II. For laminar flow the points lie on the theoretical curve, $\lambda_L = \frac{24}{Re}$, but for turbulent flow the empirical expression, $\lambda_T = \frac{0.079}{Re^{\frac{1}{4}}}$, as stated by Blasius gives values of the resistance coefficient lower than those calculated from the test results. The experimental points for turbulent flow lie close to the two curves, $\lambda_T = \frac{0.087}{Re^{\frac{1}{4}}}$ and $\lambda_T = \frac{0.081}{Re^{\frac{1}{4}}}$, the first fitting the results for h = 0.0093" and the second the results for h = 0.0058" and h = 0.0040". Except for the case where h = 0.0050", the results indicate that the smaller the value of h the closer lie the points to the empirical curve, $\lambda_T = \frac{0.079}{Re^{\frac{1}{4}}}$.

The transition from laminar to turbulent flow takes place over a range of Re which is slightly different for each slot. These ranges are given in Appendix III, the average values of Re at the beginning and at the end of transition being 2,120 and 3,810.

4.2 Case 2. Constant Depth and Increasing Width

Two slots were used, each having a constant depth, h, and an increasing width given by $c = \alpha \, . \, x$. The depth in each case was 0.0036", and the values of $\alpha$ were 0.1 and 0.2.

The axial pressure distributions are shown in Fig. 8. The analysis reveals that these are of the form

$$p^2 = A - B \; . \; \log_e x \qquad \text{for laminar flow}$$

and

$$p^2 = C + D \; . \; \frac{1}{x^{\frac{3}{4}}} \qquad \text{for turbulent flow.}$$

A, B, C, and D are constants, and x is the axial distance from the imaginary point of intersection of the two side walls. In this case the analysis is not so accurate as for case 1 and, although a straight line is obtained by plotting $p^2$ against $x^{-0.75}$, this figure cannot be taken as exact since a similar straight line may be obtained by plotting $p^2$ against $x^n$, where n ranges from 0.70 to 0.80. The slight scatter due to errors in the readings of p is sufficient to mask the small deviations from the linear obtained with the variation of n over this range.

In the first $\frac{3}{4}$" of slot length there was an appreciable divergence from the theoretical form of pressure distribution and a central 3" length was therefore chosen as the test length. A series of readings of $p_1$, $p_2$ and G were taken for each slot, where $p_1$ and $p_2$ were respectively the pressures at the upstream and at the downstream end of the test length. The values of $(p_1^2 - p_2^2)$ are plotted logarithmically against the corresponding values of G in Fig. 9 and the results are seen to lie on two inclined straight lines, thus indicating the relationship

$$p_1^2 - p_2^2 = \text{Constant} \cdot G^n$$

The index n is 1.0 for laminar flow, but for turbulent flow it differs in the two slots, being 1.85 when $\alpha = 0.1$ and 1.60 when $\alpha = 0.2$. Also shown in Fig. 9 are the corresponding theoretical curves obtained from equations (13) and (15). The theoretical curves for laminar flow are identical with the test results.

The Reynolds number, Re, being a function of the width, c, varies along the slot for any given value of G and it is not possible, therefore, to express the results as a graph of $\lambda$ against Re. For the same reason, the change from laminar to turbulent flow does not take place at the same value of G in both slots, but is determined instead by the conditions at the entry where the Reynolds number is highest. The values of Re at the entry corresponding to the beginning of the transition are 2,760 and 3,020 for $\alpha = 0.1$ and $\alpha = 0.2$ respectively. The critical value for a parallel slot of the same depth is estimated from the values in Appendix III as 2,400.

4.3 Case 3. Constant Width and Increasing Depth

Two slots of constant width equal to 1.83" were used, each having a depth given by $h = \beta \cdot x$, where $\beta$ was $0.5 \cdot 10^{-3}$ in one test and $0.67 \cdot 10^{-3}$ in the other.

Fig. 10 shows the pressure distributions, which when analysed over the central length are found to be of the form

$$p^2 = E + F \cdot \frac{1}{x^2}$$

for both laminer and turbulent flow, where E and F are constants and x is the axial distance from the imaginary line of intersection of the two planes. As in the other cases, there is a considerable divergence from the theoretical relationship in the first $\frac{3}{4}$" of the slot and a central 3" length was again chosen as the test section. Readings of $p_1$, $p_2$, and G were taken and these are plotted logarithmically in Fig. 11 as $(p_1^2 - p_2^2)$ against G. As in the previous cases the relationship between the pressure drop and the mass flow is of the form

$$p_1^2 - p_2^2 = \text{Constant} \cdot G^n$$

The index n is 1.0 for laminar flow and 1.75 for turbulent flow.

The theoretical and empirical curves obtained from equations (17) and (19) are also shown in Fig. 11. The discrepancy between the test results and the theoretical curves for laminar flow is unexpected, since all previous laminar results have been in close agreement with the theory. For this reason an error in the calculation of $\beta$ was suspected and it is shown in Appendix IV that a difference of 10% in the theoretical value of $(p_1^2 - p_2^2)$ may be due to a difference in $\beta$ of less than 4%. The discrepency may, therefore, be due to an error in the measurement of h of only 0.0002", an error which is quite possible with the stepped shims used in this case. The laminar results were accordingly assumed to be correct and new values of $\beta$ calculated.

Using the corrected values of $\beta$, $\lambda_T$ and Re were calculated from the equations in Appendix III and are plotted in Fig. 12. The turbulent results lie on two curves, $\lambda_T = \frac{0.063}{Re^{\frac{1}{4}}}$ and $\lambda_T = \frac{0.067}{Re^{\frac{1}{4}}}$, for $\beta = 0.64 \times 10^{-3}$ and

$\beta = 0.49 \times 10^{-3}$ respectively. It appears that the constant $(\lambda_T \cdot Re^{\frac{1}{4}})$ may be dependent upon the slot divergence and so it is plotted against $\beta$ in Fig. 13. Since the mean depth of the two slots used, in this case was less than 0.006" (see section 4.1.), the value of $(\lambda_T \cdot Re^{\frac{1}{4}})$ corresponding to $\beta = 0$ (Case 1.) was taken as 0.081. Fig. 13 shows that the three points lie approximately on a straight line, thus indicating a possible relationship between $\lambda_T$, Re, and $\beta$ of the form

$$\lambda_T = \frac{0.81 - 28\,\beta}{Re^{\frac{1}{4}}}$$

However, further tests will be necessary to verify this hypothesis.

## 5.0 Conclusions

The comparison of the test results with the corresponding theoretical and empirical relationships shows that these relationships hold approximately for the flow of air in any narrow slot, provided that the divergence is small and that the length considered does not lie within about $\frac{3}{4}$" of the slot entry or the slot exit. With these provisions the forces due to the changes in kinetic energy are negligible, so that the assumption made in developing the theory is valid.

The results also indicate that the theoretical equations may be used to give an accurate quantitative description of laminar flow. The only serious discrepancy between the theory and the test results was in the case of the slots with increasing depth and here the error was assumed to be in the measurement of the divergence.

For turbulent flow the empirical relationships based on the value of the resistance coefficient given by Blasius, $\lambda_T = \frac{0.079}{Re^{\frac{1}{4}}}$, are not in general applicable. The investigation shows that for slots of constant cross section the actual value of $\lambda_T$ is larger, being $\frac{0.087}{Re^{\frac{1}{4}}}$ for the slot of depth $h = 0.0093"$ and $\frac{0.081}{Re^{\frac{1}{4}}}$ for $h = 0.0058"$. For slots of increasing depth the product $(\lambda_T \cdot Re^{\frac{1}{4}})$ appears to be a constant, the value of which depends upon the rate of divergence, $\beta$, of the walls.

List of Illustrations


Fig. 1 Viscid Flow Theory.

Fig. 2 The Types of Slot Considered.

Fig. 3 The Test Block.

Fig. 4 Pressure Distribution in the Slot (Case 1).

Fig. 5 Effect of Pressure Drop on Mass Flow (Case 1).

Fig. 6 Comparison with Theory. (Case 1).

Fig. 7 Scale Effect in Case 1.

Fig. 8 Pressure Distribution in the Slot (Case 2).

Fig. 9 Effect of Pressure Drop on Mass Flow (Case 2).

Fig.10 Pressure Distribution in the Slot (Case 3).

Fig.11 Effect of Pressure Drop on Mass Flow (Case 3).

Fig.12 Scale Effect in Case 3.

Fig.13 The Effect of Slot Divergence.

Fig.14 Mach Number Variation

## List of Appendices


| | |
|---|---|
| Appendix I | List of Symbols Used. |
| Appendix II | The Calculation of λ and Re. |
| Appendix III | Transition Values of Re. |
| Appendix IV | The Effect of Errors in the Measurement of β. |


## References


| No. | Author | Title |
|---|---|---|
| 1. | N.A.V. Piercy | Aerodynamics: pp. 278; E.U.P.: 1937. |

# APPENDIX I

## List of Symbols Used

$p$ = absolute pressure

$\rho$ = density

$T$ = absolute temperature

$\mu$ = coefficient of absolute viscosity

$\nu$ = coefficient of kinematic viscosity

$\alpha$ = width of slot

$h$ = depth of slot

$l$ = length of test section

$G$ = mass flow

$\dot{Q}$ = volume of flow

$\overline{u}$ = mean velocity $= \dfrac{Q}{\alpha \, . \, h}$

$\tau$ = surface friction

$\lambda$ = resistance coefficient $= \dfrac{\tau}{\dfrac{\rho \, \overline{u}^2}{2}}$

$Re$ = Reynolds number $= \dfrac{2 \, . \, h \, . \, \overline{u}}{\nu}$

## APPENDIX II

### The Calculation of λ and Re

The calculation of the Reynolds number, Re, from the test results is based on the formula

$$Re = \frac{4m \cdot \bar{u}}{\nu}$$

where $m$ = the mean hydraulic depth,

$\bar{u}$ = the mean velocity,

and $\nu$ = the kinematic viscosity.

For a slot of rectangular cross section where h, the depth, is negligible compared with $\alpha$, the width,

$$m = \frac{\text{Area}}{\text{Perimeter}} = \frac{\alpha \cdot h}{2\alpha} = \frac{h}{2}$$

$$\text{and } Re = \frac{2 \cdot h \cdot \bar{u}}{\nu}$$

Also the mass flow, G, is given by

$$G = \rho \cdot \bar{u} \cdot \alpha \cdot h$$

$$\text{and } \nu = \mu/\rho$$

$$\text{Therefore} \quad Re = \frac{2\rho \cdot h \cdot \bar{u}}{\mu}$$

$$\text{That is} \quad Re = \frac{2G}{\alpha \cdot \mu} \qquad \text{.................(20)}$$

---

From consideration of an elementary volume of air between the two plates equation (6) is derived in section 2.2. This gives

$$\frac{dp}{dx} = -\frac{\lambda \cdot \rho \cdot \bar{u}^2}{h}$$

which, since $G = \rho \cdot \bar{u} \cdot \alpha \cdot h$, becomes

$$dp = -\frac{\lambda \cdot G^2}{\rho \cdot \alpha^2 \cdot h^3} dx$$

and, replacing $\rho$ by $\frac{p}{RT}$, we have

$$p \cdot dp = -\frac{\lambda \cdot RT \cdot G^2}{\alpha^2 h^3} \cdot dx \qquad \text{...................(21)}$$

Assuming that λ can be expressed as a function of Re, which is independent of x when $\alpha$ is constant, and that the temperature, T, is constant this equation can be integrated to give

$$p_1^2 - p_2^2 = \frac{2\lambda \cdot RT \cdot G^2 \cdot (x_2 - x_1)}{\alpha^2 \cdot h^3}$$

and hence

$$\lambda = \frac{p_1^{\,2} - p_2^{\,2}}{x_2 - x_1} \cdot \frac{\alpha^2\, h^3}{2\, RT \, . \, G^2} \qquad \ldots\ldots\ldots\ldots(22)$$

For case 3, in which the depth of the slot is increasing, we can obtain a corresponding equation for $\lambda$ by substituting $h = \beta x$ in equation (21) and by integrating.

This is $p \,.\, dp = - \dfrac{\lambda \,.\, RT \,.\, G^2}{\alpha^2\, \beta^3} \cdot \dfrac{dx}{x^3}$

and $\quad p_1^{\,2} - p_2^{\,2} = \dfrac{\lambda \,.\, RT \,.\, G^2}{\alpha^2\, \beta^3} \left(\dfrac{1}{x_1^{\,2}} - \dfrac{1}{x_2^{\,2}}\right)$

Hence

$$\lambda = \frac{p_1^{\,2} - p_2^{\,2}}{\left(\frac{1}{x_1^{\,2}} - \frac{1}{x_2^{\,2}}\right)} \cdot \frac{\alpha^2 \,.\, \beta^3}{RT \,.\, G^2} \qquad \ldots\ldots\ldots\ldots\ldots\ldots(23)$$

## APPENDIX III

### Transition Values of $R_e$

The range of mass flow over which transition from laminar to turbulent flow takes place is slightly different for each slot.

The following table gives the approximate transition range of mass flow for each test, together with the corresponding range of $R_e$ calculated from the relation

$$Re = \frac{2 \cdot G}{a \cdot \mu}$$

| Depth, h inches. | Range of G lbs./sec. | $\mu$ lb/ft. sec. | Range of Re |
|---|---|---|---|
| 0.0030 | $(22.9 - \quad) \cdot 10^{-4}$ | $1.189 \cdot 10^{-5}$ | 2,640 - * |
| 0.0040 | $(20.0 - 28.8) \cdot 10^{-4}$ | $1.198 \cdot 15^{-5}$ | 2,290 - 3,290 |
| 0.0050 | $(16.6 - 37.2) \cdot 10^{-4}$ | $1.201 \cdot 10^{-5}$ | 1,890 - 4,250 |
| 0.0058 | $(17.38 - 36.3) \cdot 10^{-4}$ | $1.198 \cdot 10^{-5}$ | 1,990 - 4,150 |
| 0.0093 | $(15.9 - 31.6) \cdot 10^{-4}$ | $1.225 \cdot 10^{-5}$ | 1.780 - 3,540 |

The mean values of Re for the beginning and the end of transition are 2,120 and 3,810 respectively.

*With the available air supply it was not possible to obtain turbulent flow in the slot having a depth of 0.0030" and the higher limits of transition cannot, therefore, be given in this case.

## APPENDIX IV

### The Effect of Errors in the Measurement of $\beta$

Fig. 13b shows a section through a slot of increasing depth, showing h' and h" the clearances which define the divergence, $\beta$. The depth, h, was assumed to be equal to the thickness of the steel shim at the point considered as measured by a micrometer.

When $p^2$ is plotted against $\frac{1}{x^2}$ a straight line is obtained and the values of x are therefore assumed to be correct. The point O is then fixed, the errors which occur being in the calculation of the angle COA.

The theoretical and empirical equations for slots of this kind are

$$p_1^2 - p_2^2 = \frac{12\,\mu\,.\,RT\,.\,G}{\sigma\,.\,\beta^3}\left\{\frac{1}{x_1^2} - \frac{1}{x_2^2}\right\} \text{ for laminar flow,}$$

and

$$p_1^2 - p_2^2 = \frac{0.067\,\mu^{\frac{1}{4}}\,.\,RT\,.\,G^{\frac{7}{4}}}{\sigma^{\frac{7}{4}}\,.\,\beta^3}\left\{\frac{1}{x_1^2} - \frac{1}{x_2^2}\right\} \text{ for turbulent flow.}$$

An error in the measurement of h gives a false value of $\beta$ which, since it occurs in the equations at $\beta^3$, gives a very large error in the theoretical value of $(p_1^2 - p_2^2)$.

Consider the case where the measured values of h are

$$h' = 2.0''.\,10^{-3} \qquad h'' = 6.0''.\,10^{-3}$$

Then

$$\beta = \frac{h'' - h'}{x'' - x'} = \frac{4\,.\,10^{-3}}{6} = 0.667\,.\,10^{-3}$$

Suppose that the actual values of h are

$$h' = 1.933''.\,10^{-3} \qquad h'' = 5.8''.\,10^{-3}$$

Then $\beta^{*}$(the real value) $= \frac{h'' - h'}{x'' - x'} = \frac{3.867}{6}\,.\,10^{-3} = 0.645\,.\,10^{-3}$

Hence

$$\left(\frac{\beta}{\beta^{*}}\right) = \frac{4.000}{3.867} \doteqdot 1.034$$

$$\left(\frac{\beta}{\beta^{*}}\right)^3 \doteqdot 1.11$$

The resulting error in $(p_1^2 - p_2^2)$ is, therefore, 11% and is due to a maximum error, $\delta h''$, of only 0.0002".

FIG. 1.

# VISCID FLOW THEORY

(a) ELEMENTARY VOLUME OF FLUID

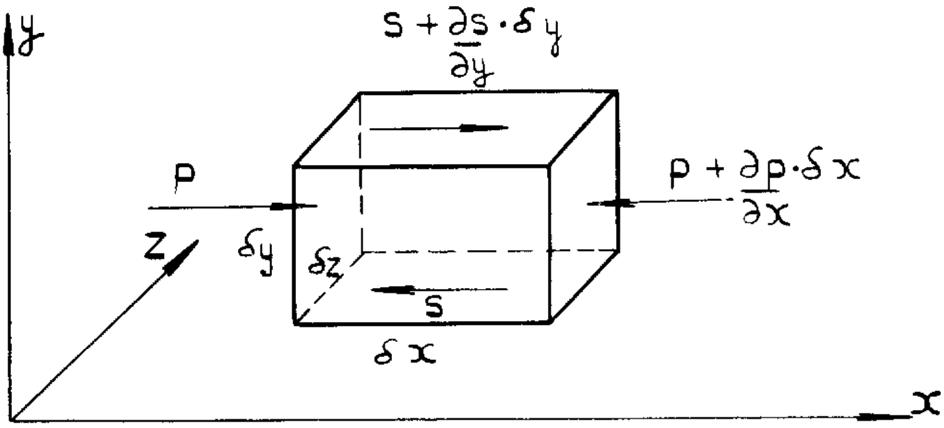


(b) ELEMENTARY VOLUME BETWEEN TWO PLATES

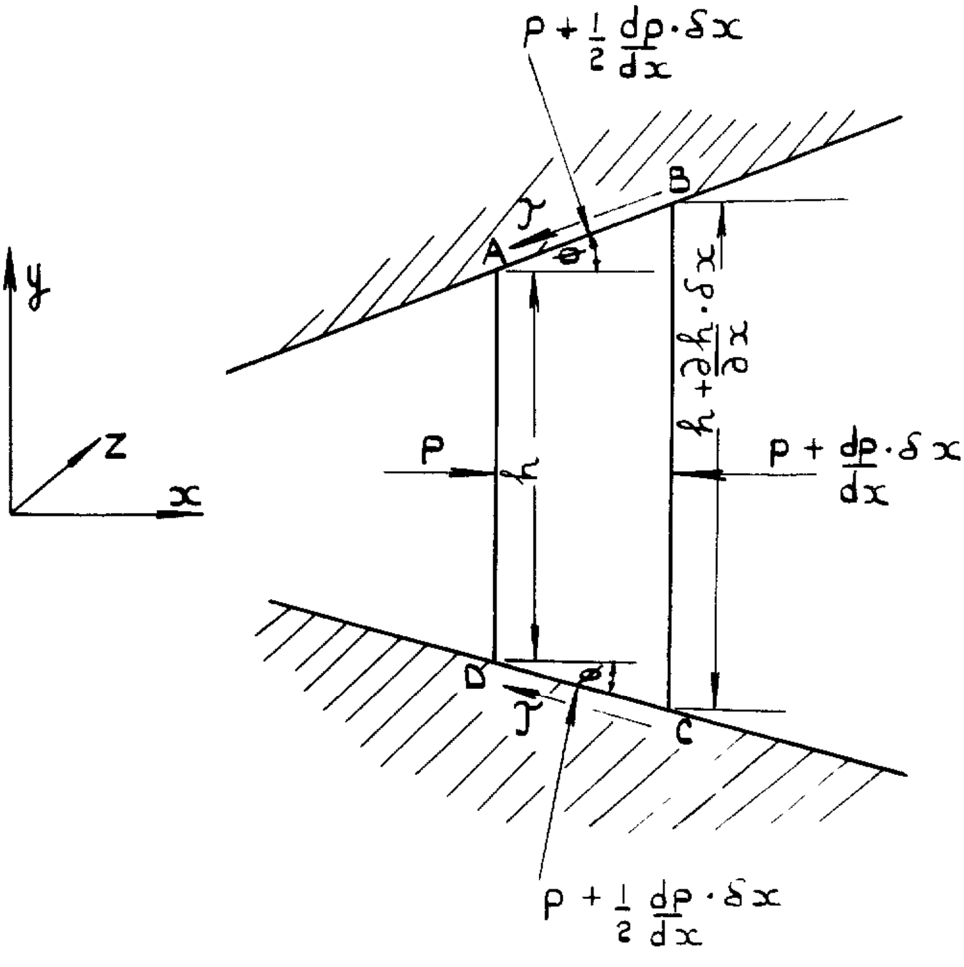

FIG. 2.

# THE TYPES OF SLOT CONSIDERED.

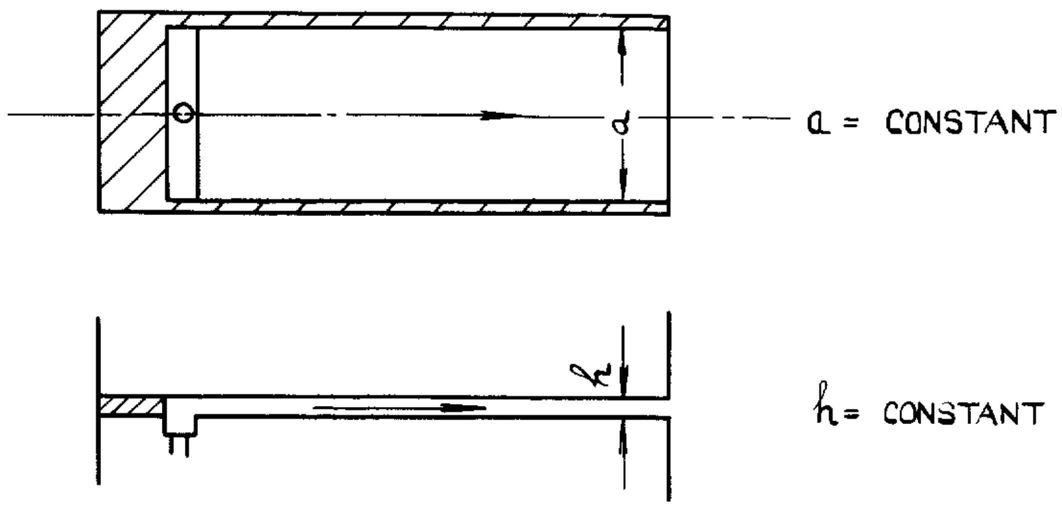


(a) CASE 1 CONSTANT CROSS SECTION

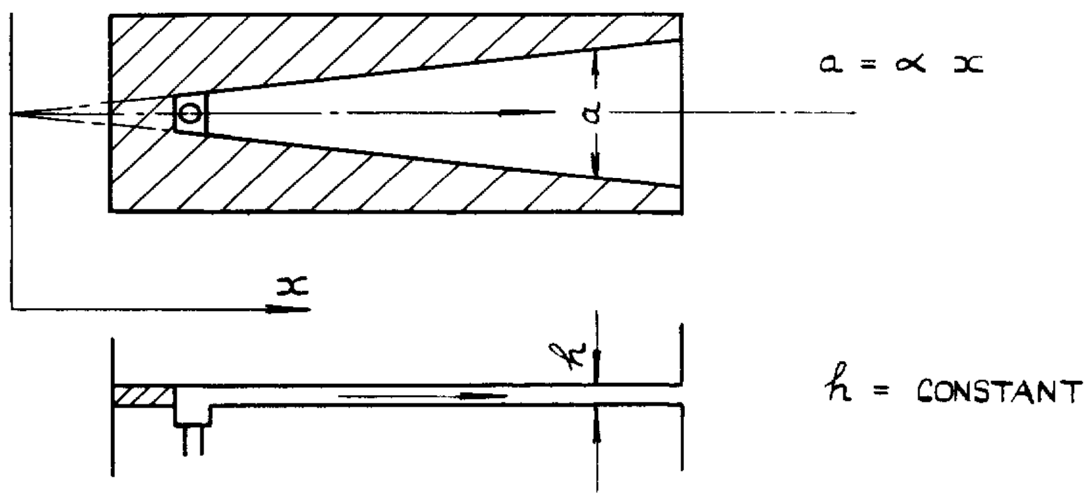


(b) CASE 2 INCREASING WIDTH

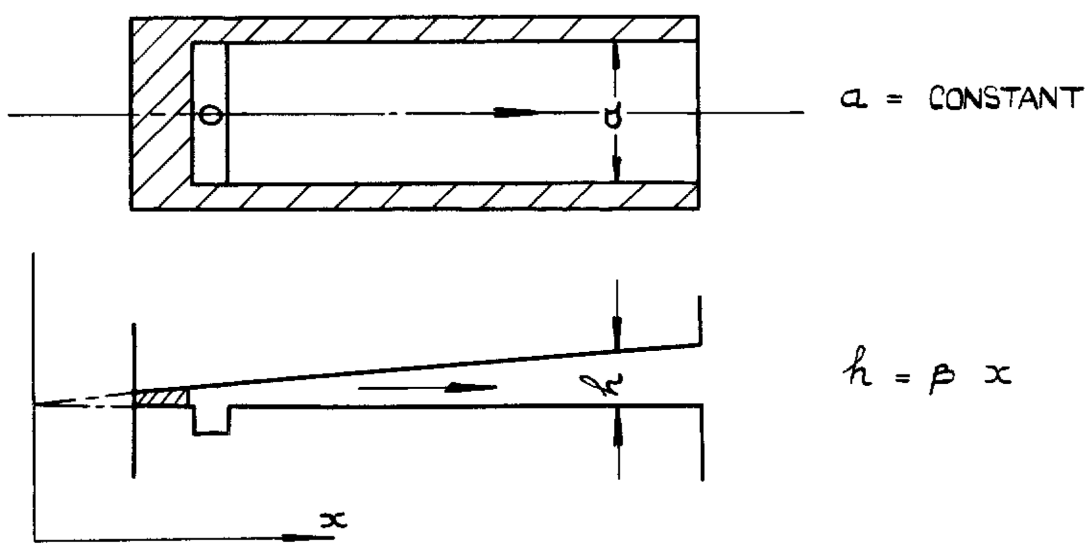


(c) CASE 3 INCREASING DEPTH

FIG.3.

# THE TEST BLOCK.

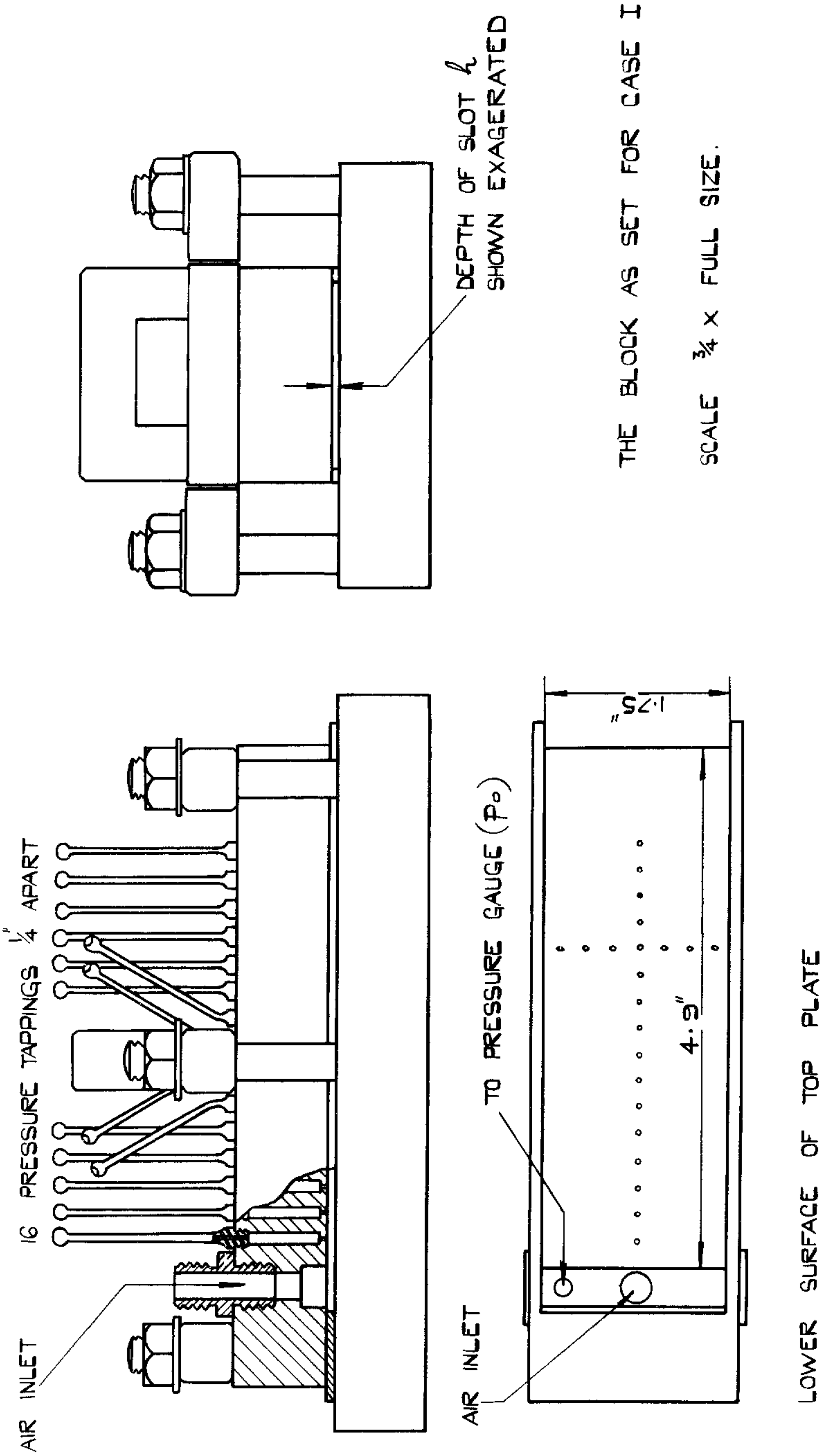

FIG 4.

# PRESSURE DISTRIBUTION IN THE SLOT.

(CASE 1: CONSTANT CROSS SECTION, $a = 1{\cdot}75''$)

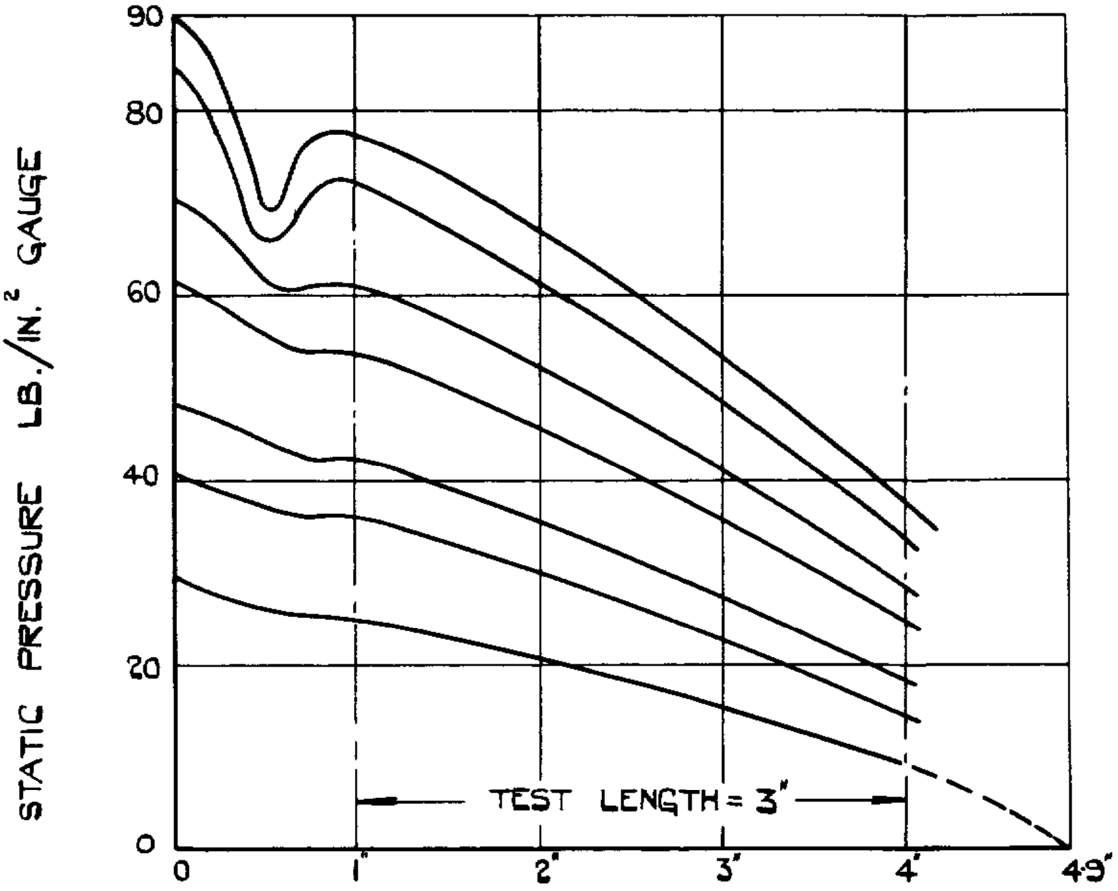


DISTANCE FROM RESERVOIR – INCHES

(a) DEPTH $h$ = 0·0020"

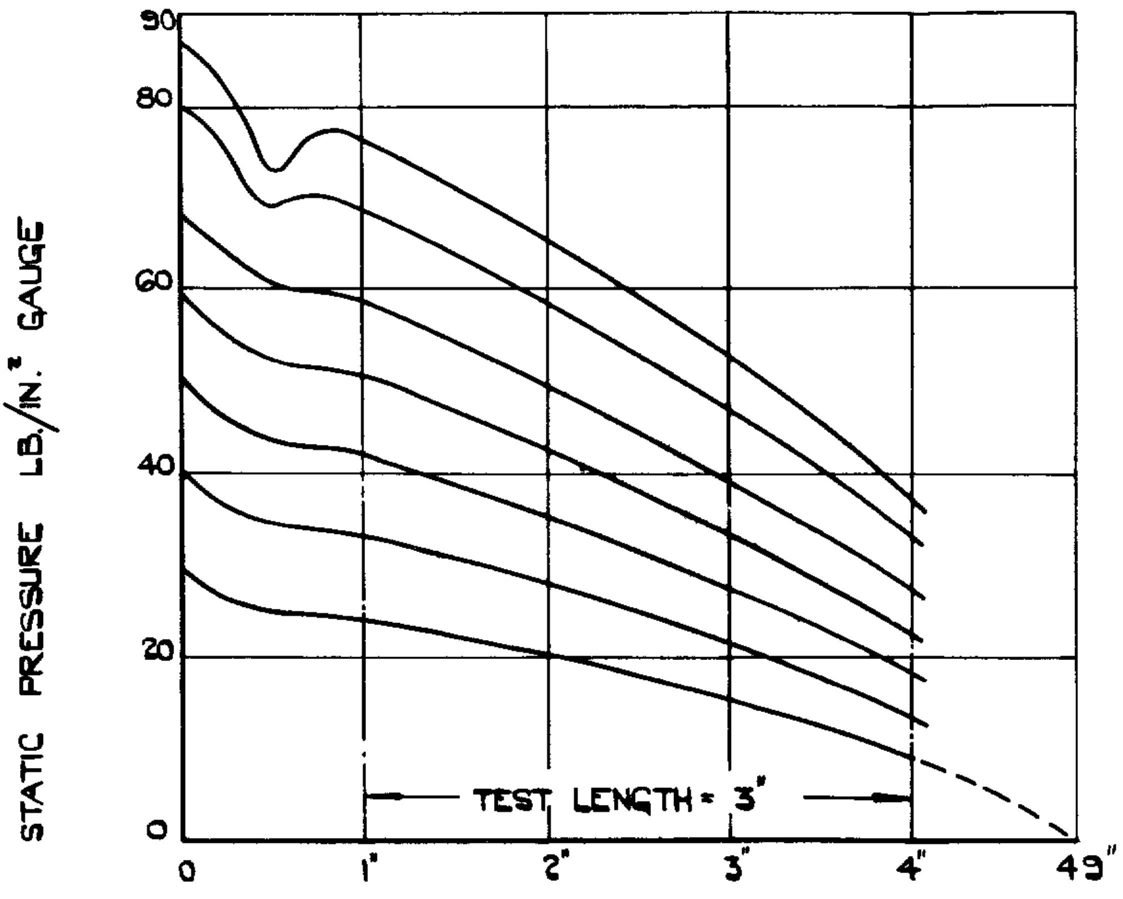


DISTANCE FROM RESERVOIR – INCHES

(b) DEPTH $h$ = 0·0050"

FIG. 5.

# EFFECT OF PRESSURE DROP ON MASS FLOW.

(CASE 1: CONSTANT CROSS SECTION, $a = 1 \cdot 75''$)

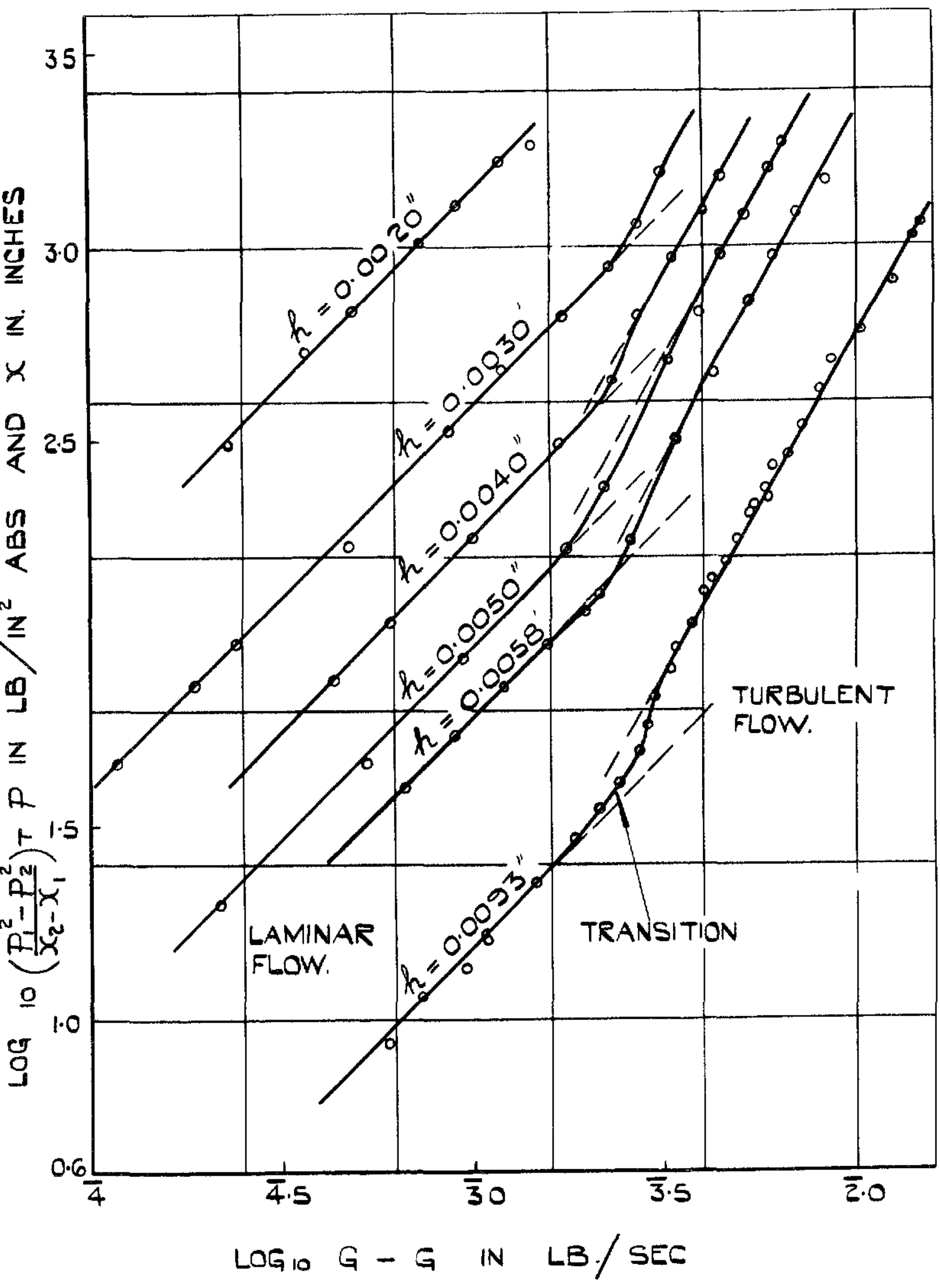

FIG. 6.

# COMPARISON WITH THEORY.

(CASE 1 : CONSTANT CROSS SECTION, $a = 1{\cdot}75''$)

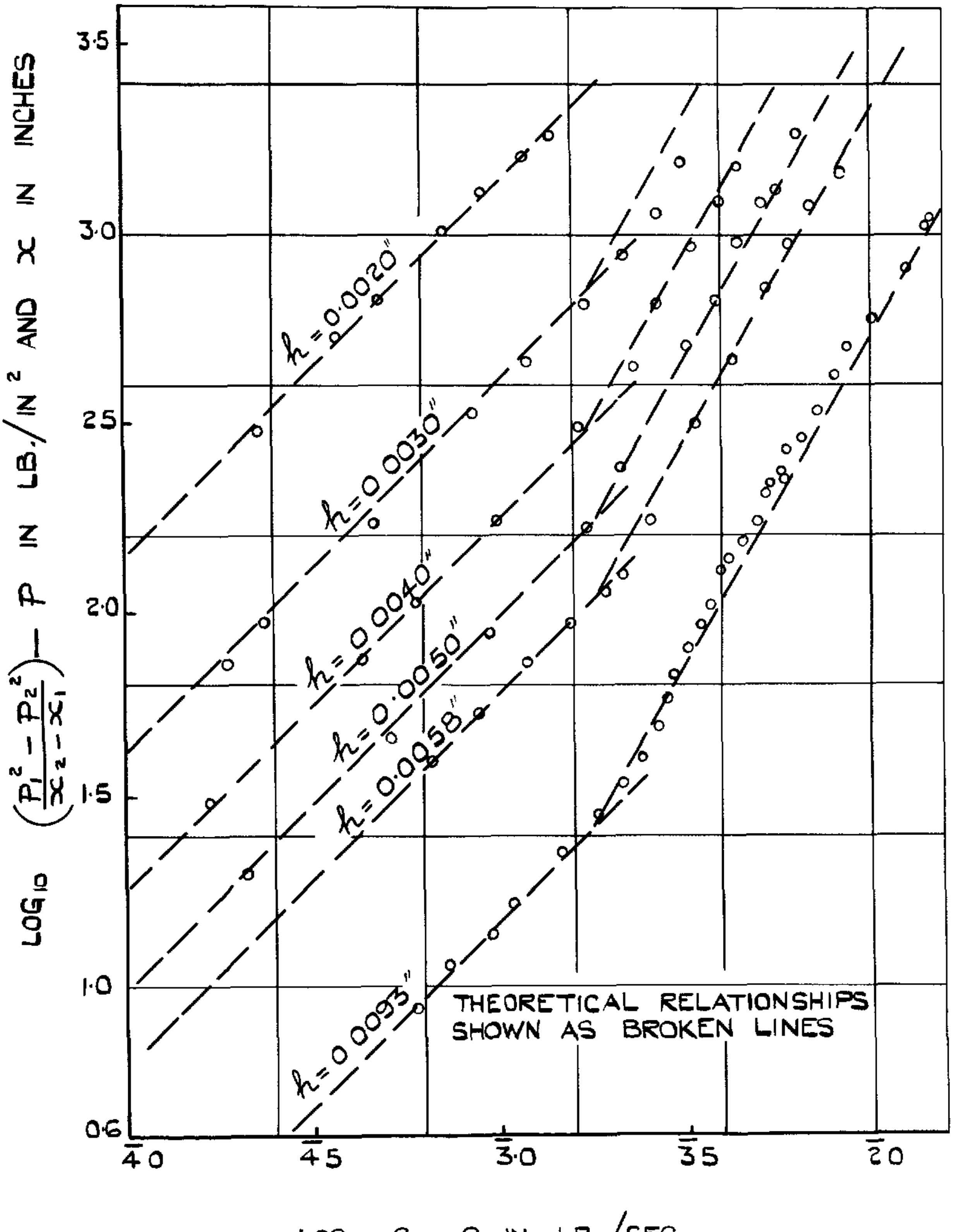

FIG. 7.

## SCALE EFFECT IN CASE I.

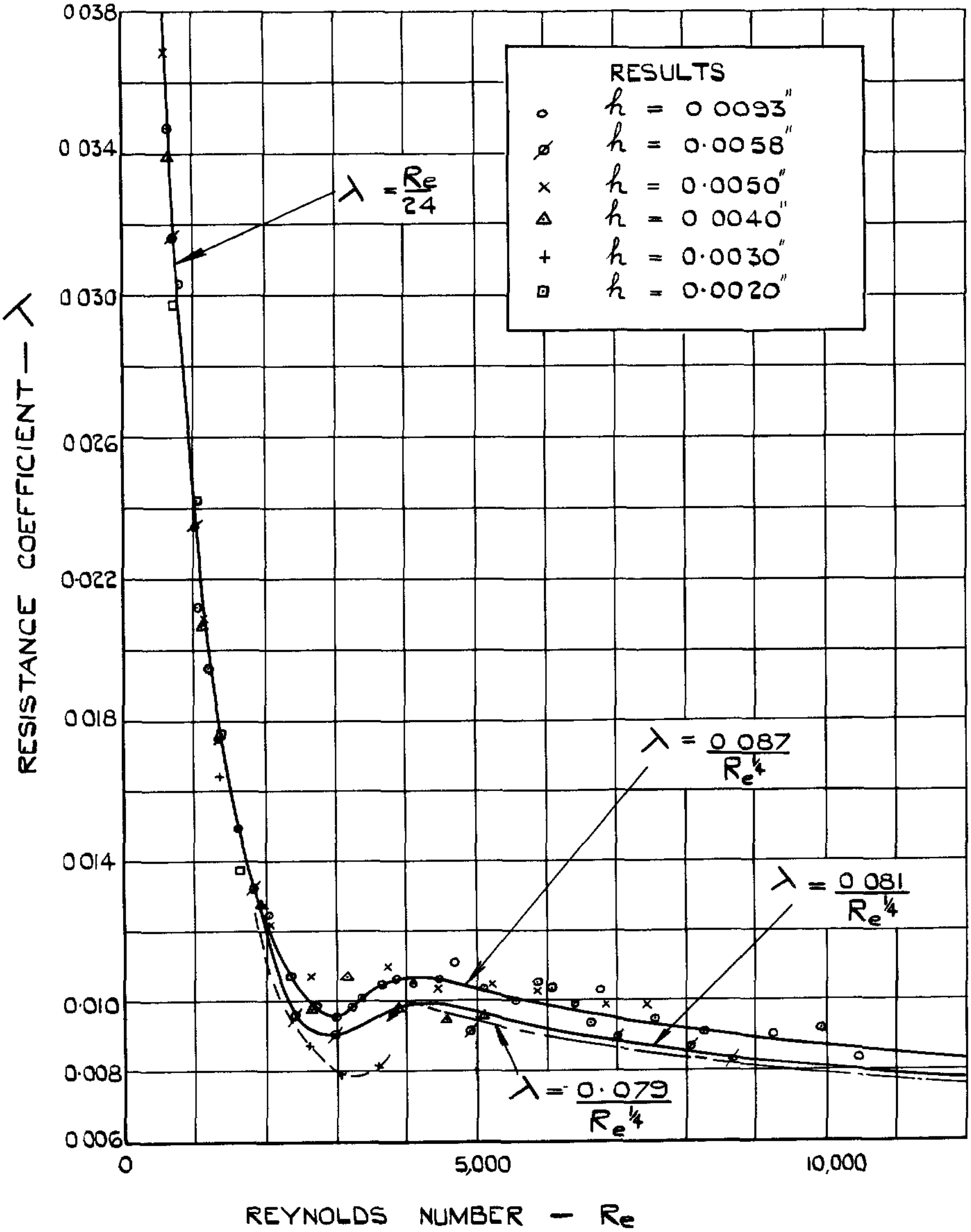

FIG. 8.

# PRESSURE DISTRIBUTION IN THE SLOT.

(CASE 2: CONSTANT DEPTH, $h = 3{\cdot}6'' \times 10^{-3}$, $a = \alpha \cdot x$)

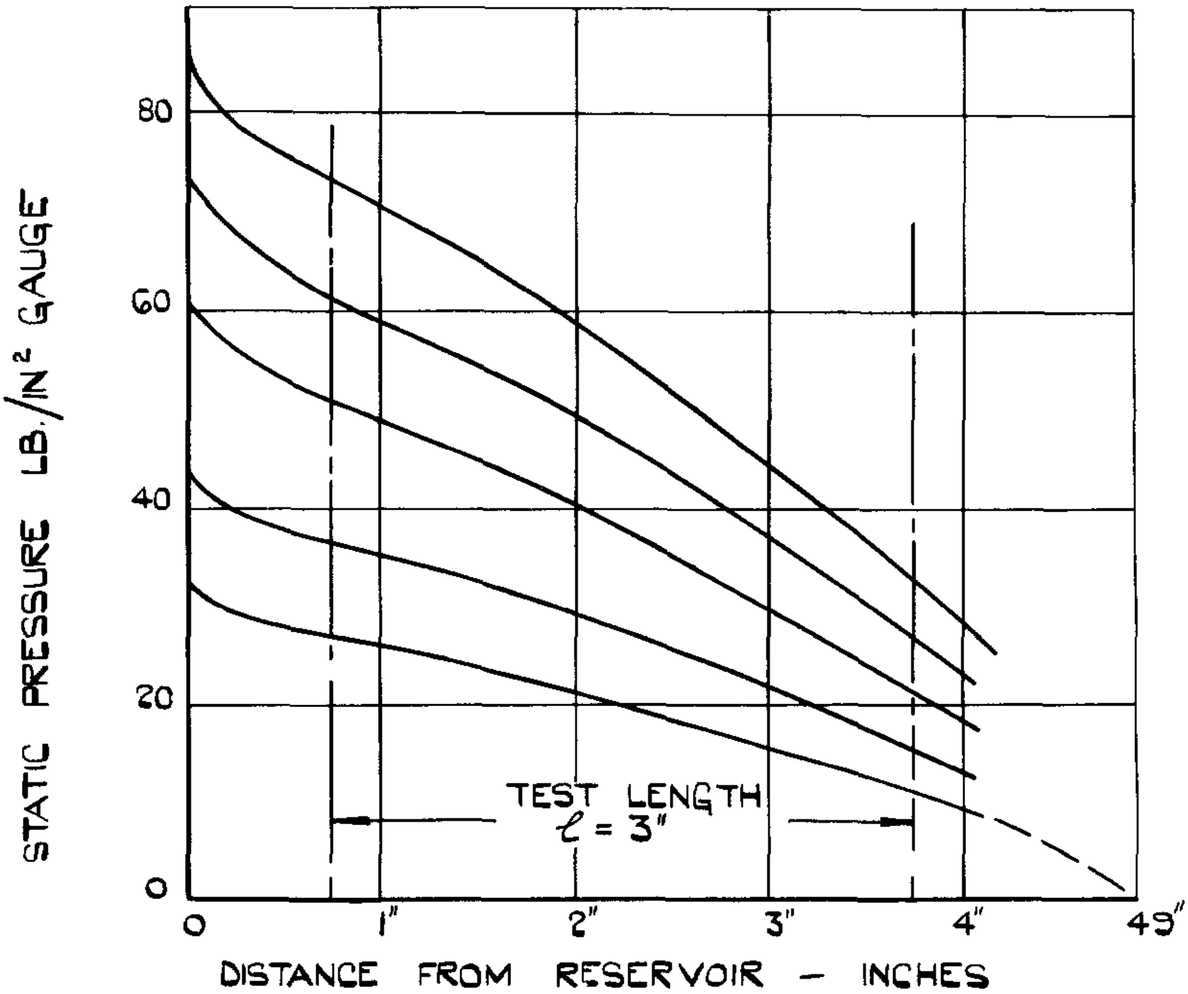


(a) WIDTH INCREASING – $\alpha = 0{\cdot}1$

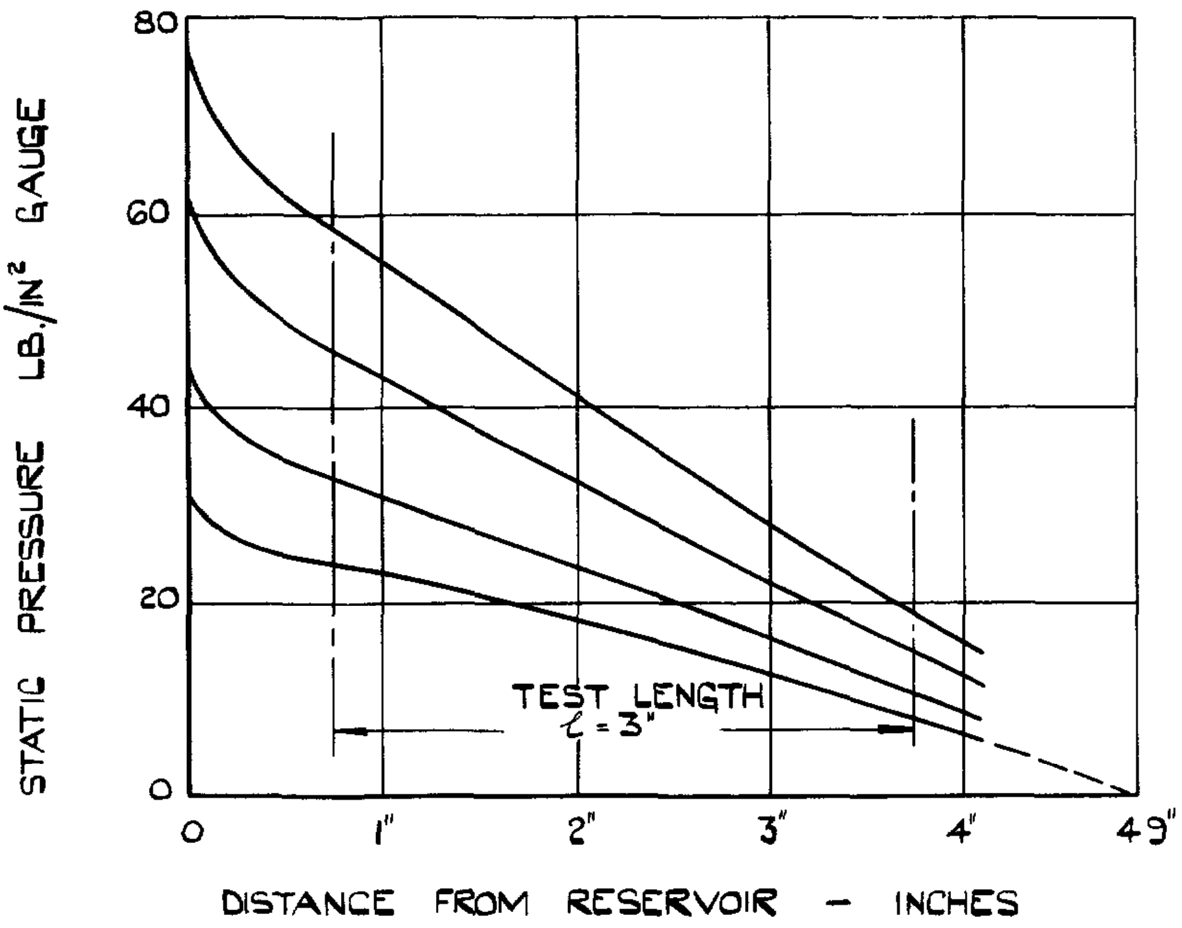


(b) WIDTH INCREASING – $\alpha = 0{\cdot}2$

FIG. 9.

# EFFECT OF PRESSURE DROP ON MASS FLOW

CASE 2: CONSTANT DEPTH, $h = 3{\cdot}6'' \times 10^{-3}$, $a = \alpha \cdot x$

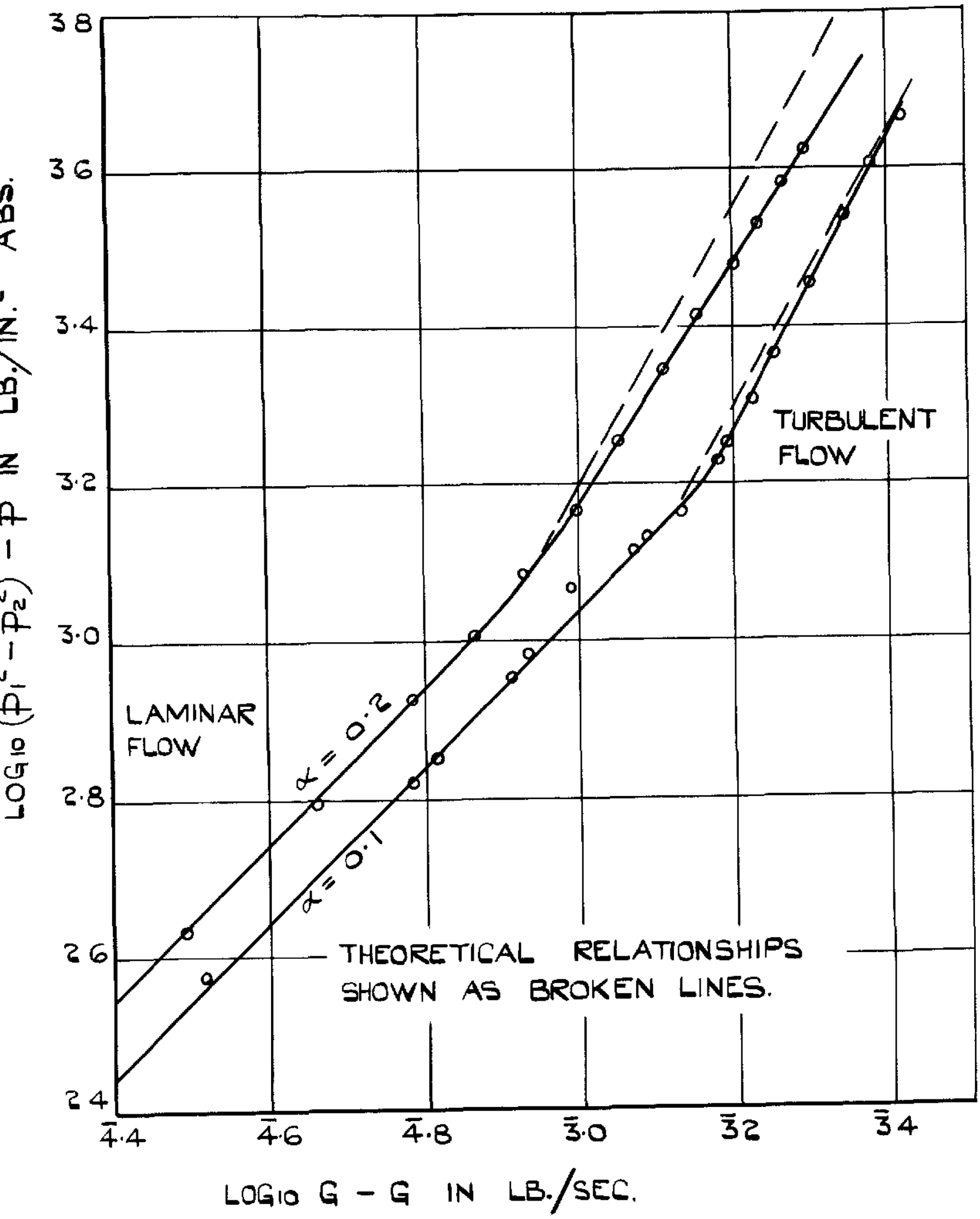

FIG 10.

# PRESSURE DISTRIBUTION IN THE SLOT.

(CASE 3: CONSTANT WIDTH, $a = 1{\cdot}83''$, $h = \beta \cdot x$)

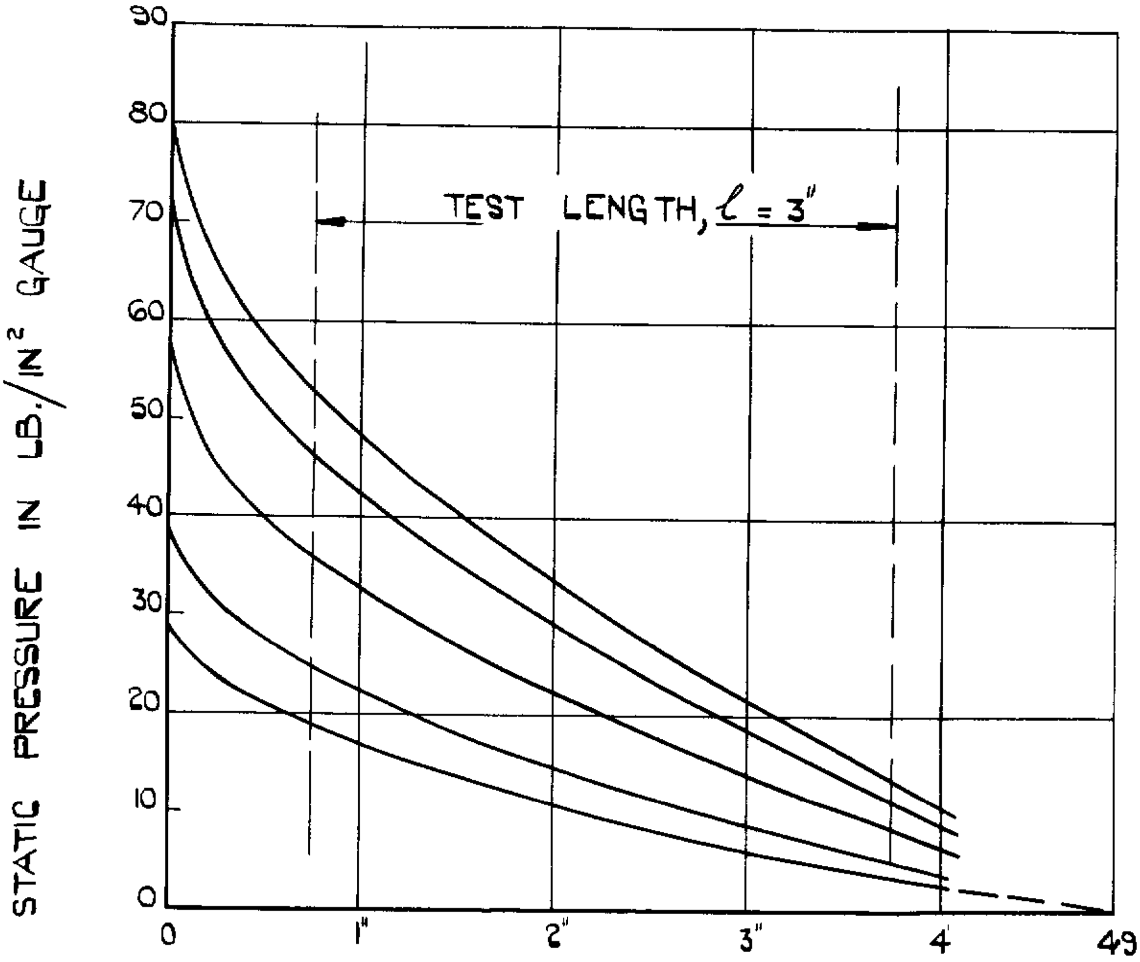


(a) INCREASING DEPTH – $\beta = 0{\cdot}5 \times 10^{-3}$

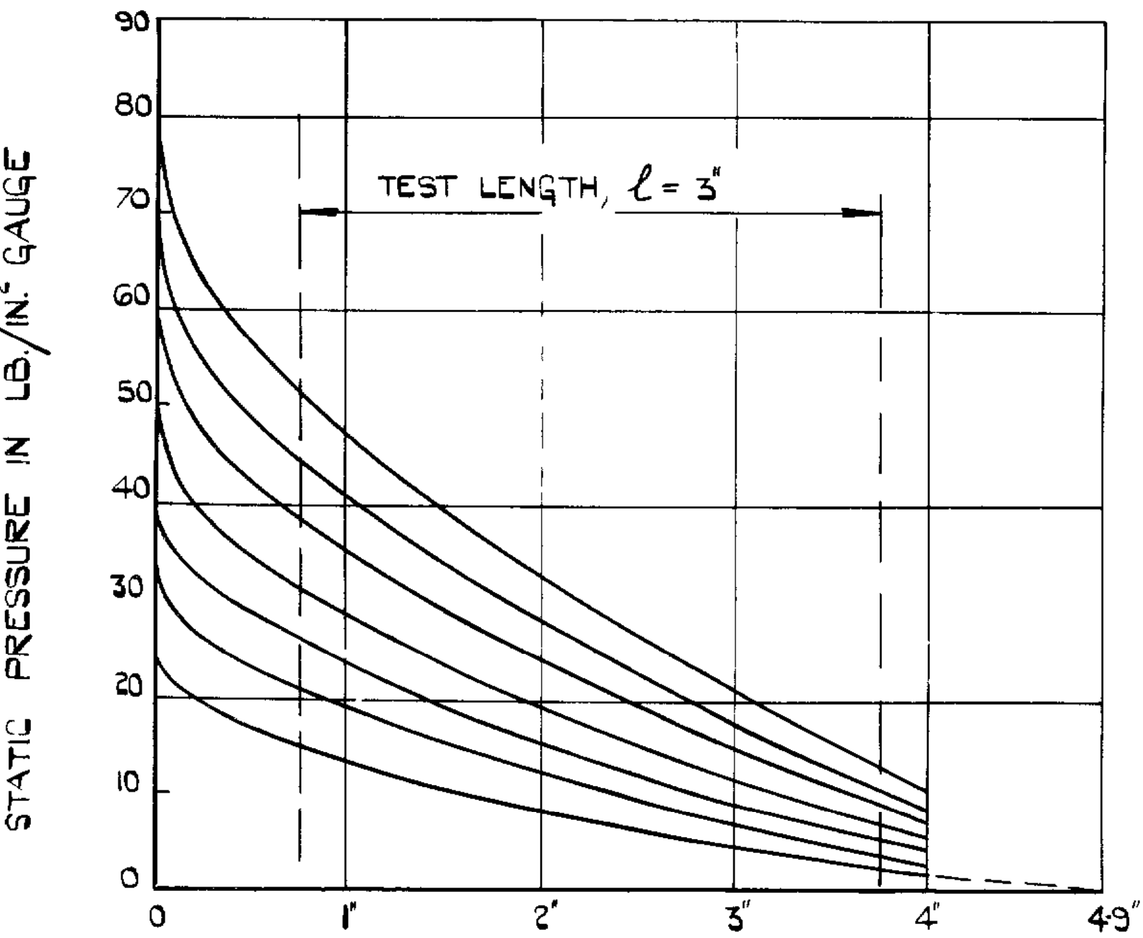


(b) INCREASING DEPTH – $\beta = 0{\cdot}67'' \times 10^{-3}$

FIG. 11.

# EFFECT OF PRESSURE DROP ON MASS FLOW.

(CASE 3: CONSTANT WIDTH, $a = 1{\cdot}83''$, $h = \beta \cdot x$)

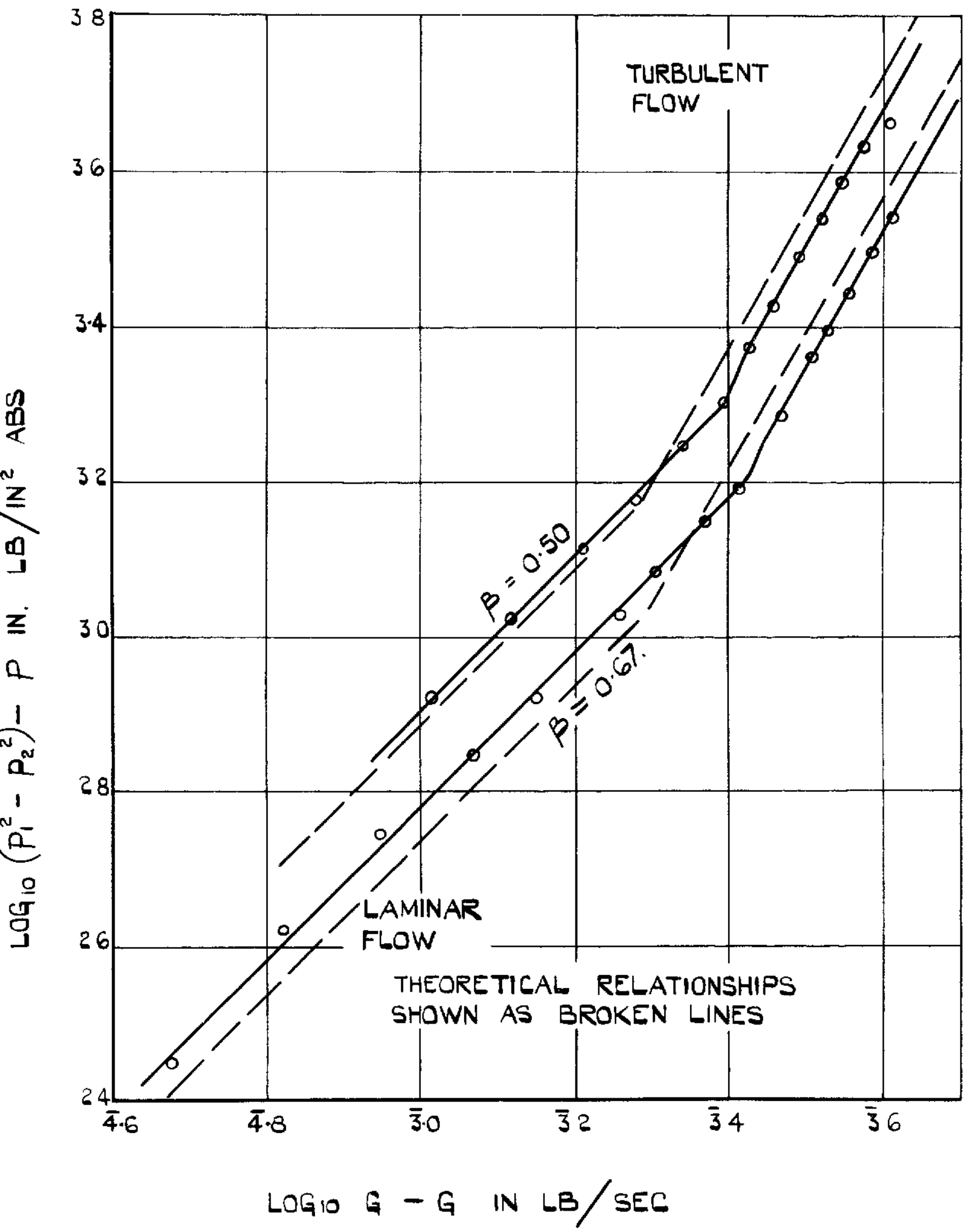

FIG. 12.

# SCALE EFFECT IN CASE 3.

(CORRECTED VALUES OF Re)

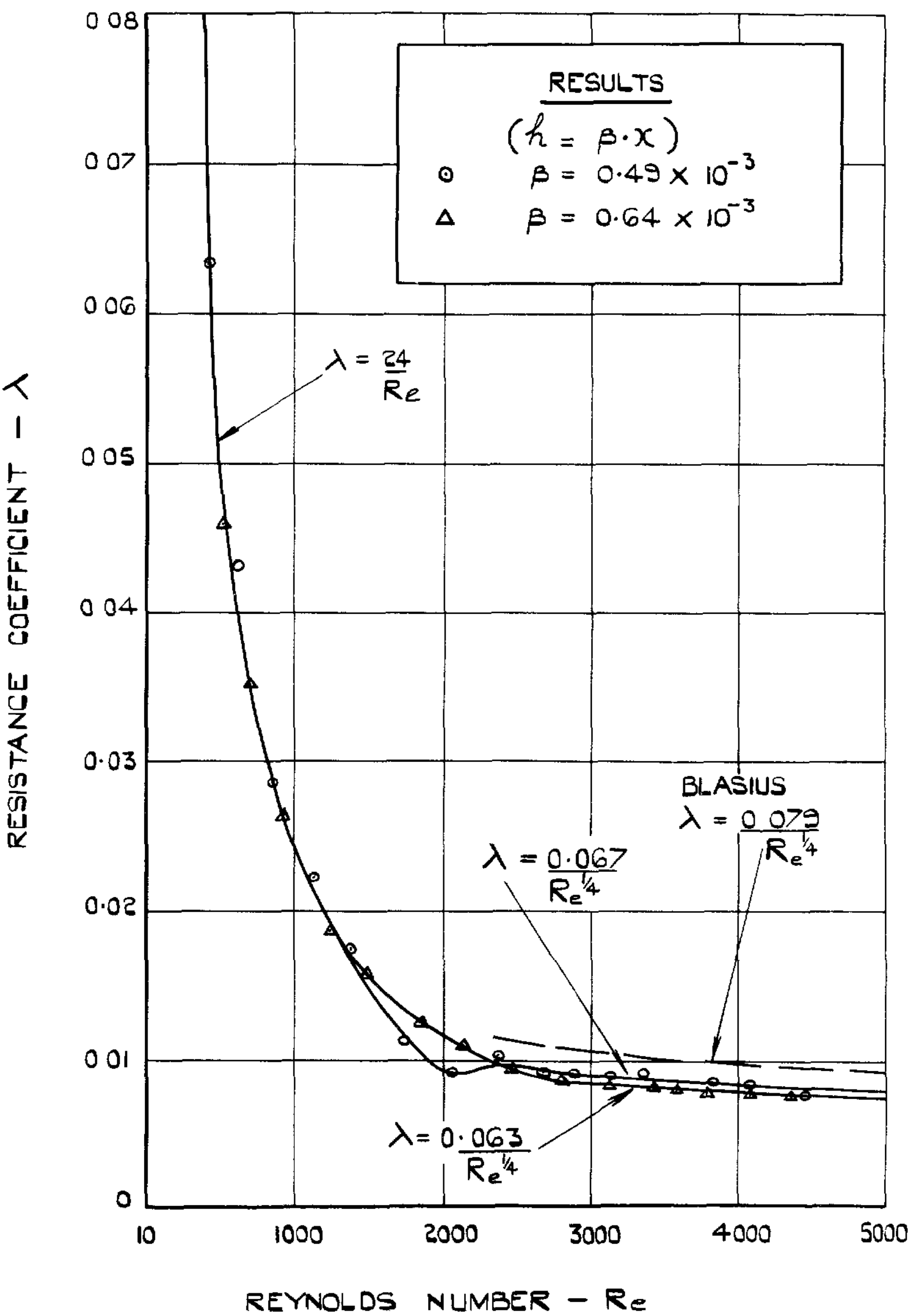

# THE EFFECT OF SLOT DIVERGENCE.

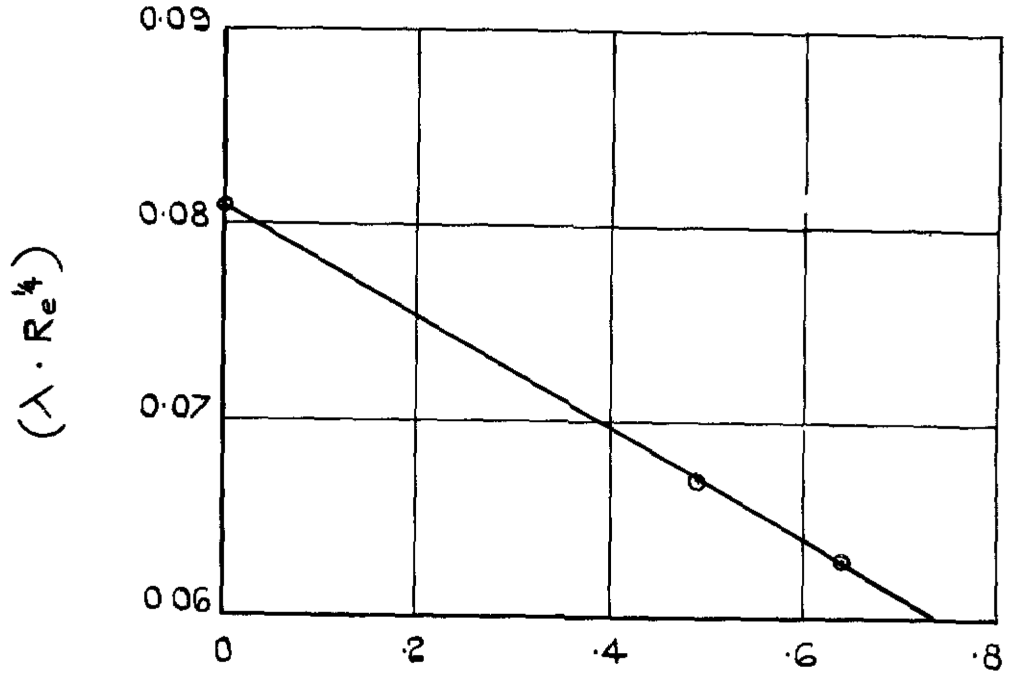


(a) VARIATION OF $(\lambda \cdot R_e^{1/4})$ WITH $\beta$

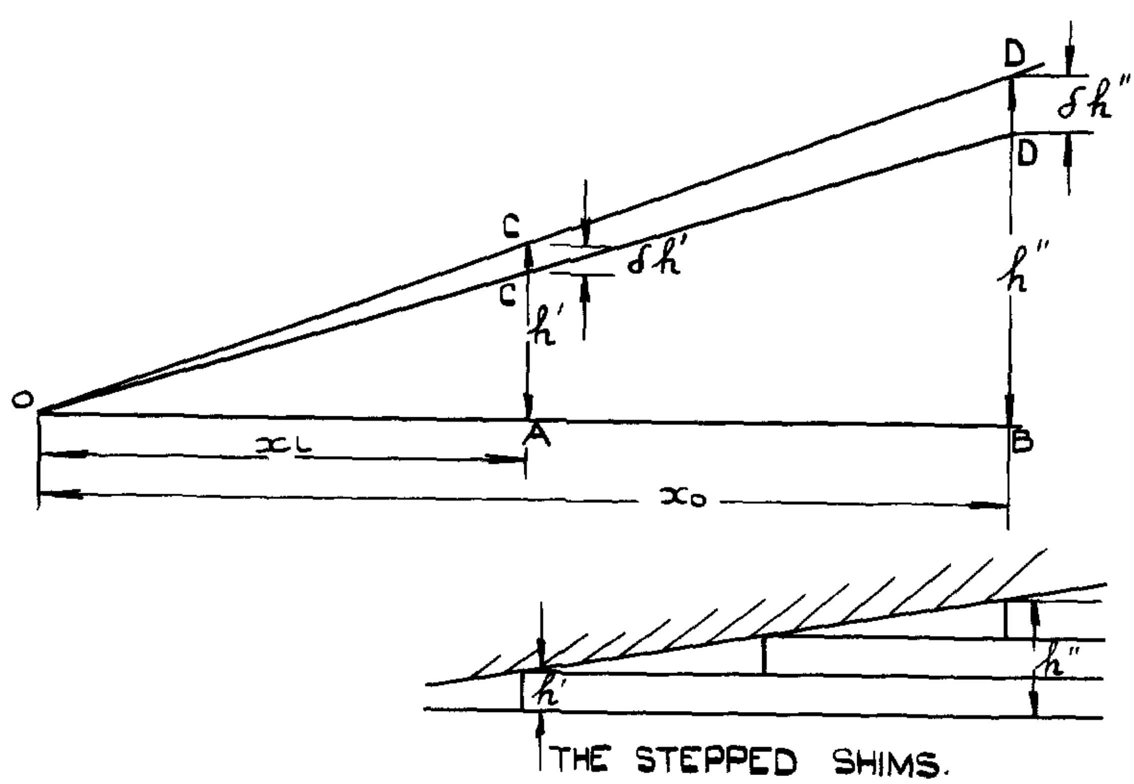


(b) THE EFFECT OF ERRORS IN THE MEASUREMENT OF $\beta$.

FIG 14.

# MACH NUMBER VARIATION.

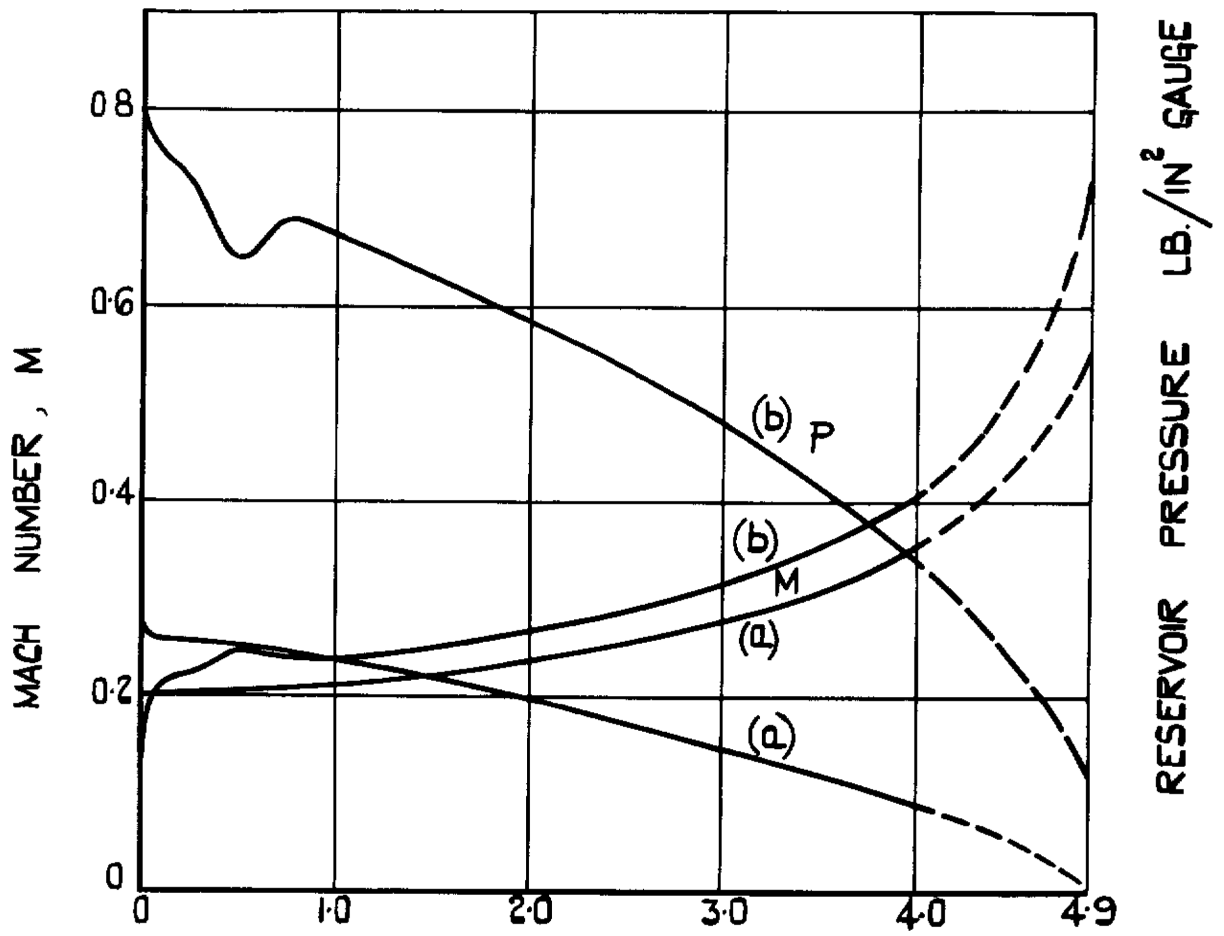


(a) VARIATION ALONG THE SLOT, $h = 5{\cdot}80 \times 10^{-3}$ IN.

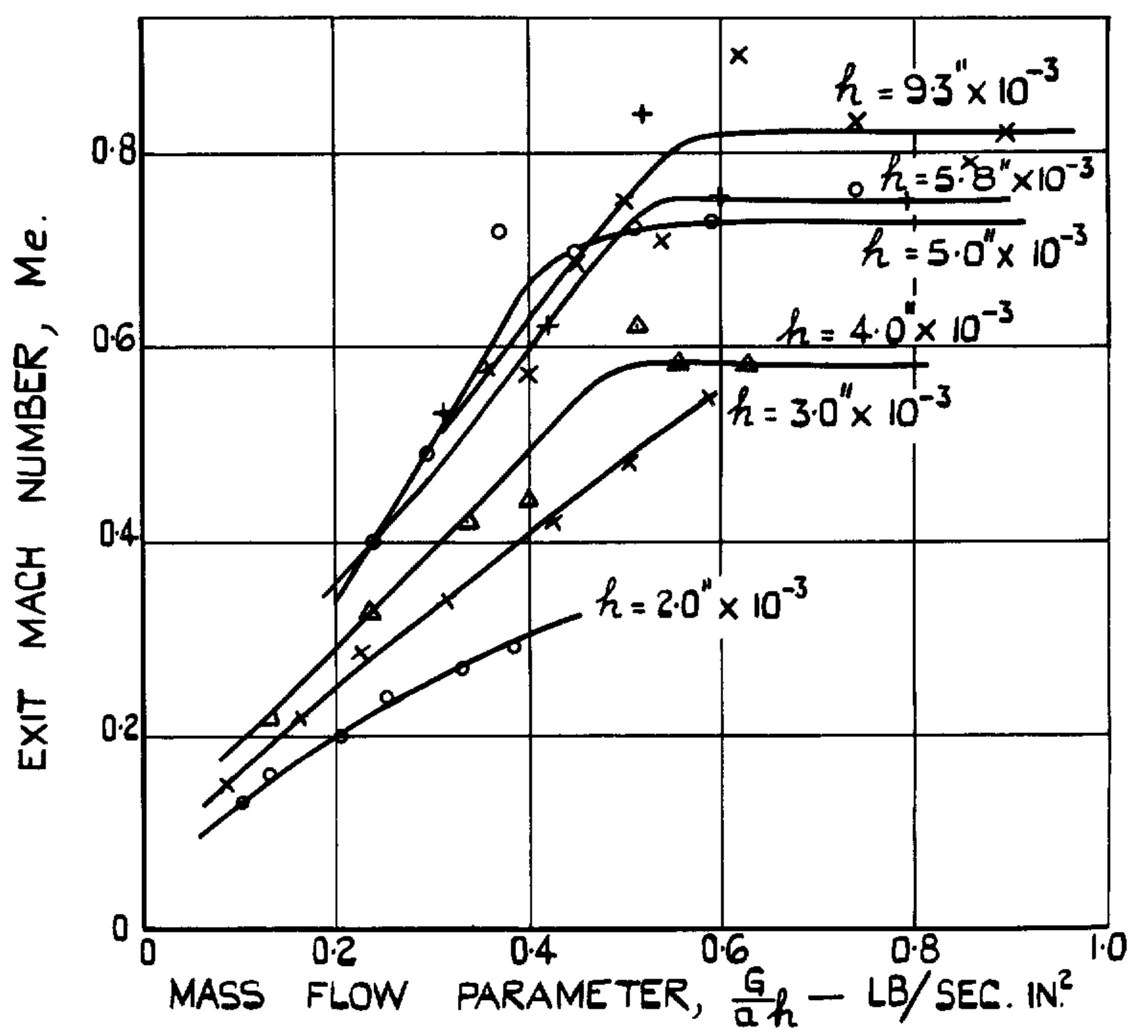


(b) EXIT MACH NUMBER

C.P. No. 13
(12329)
A.R.C. Technical Report

PRINTED AND PUBLISHED BY HIS MAJESTY'S STATIONERY OFFICE
To be purchased from
York House, Kingsway, LONDON, W.C.2 429 Oxford Street, LONDON, W 1
P.O. Box 569, LONDON, S.E.1
13a Castle Street, EDINBURGH, 2 1 St. Andrew's Crescent, CARDIFF
39 King Street, MANCHESTER, 2 1 Tower Lane, BRISTOL, 1
2 Edmund Street, BIRMINGHAM, 3 80 Chichester Street, BELFAST
or from any Bookseller

1950

Price 2s 6d net

PRINTED IN GREAT BRITAIN

S.O. Code No 23-9006-13